Neotropical Ichthyology

Original article

https://doi.org/10.1590/1982-0224-2019-0126

urn:lsid:zoobank.org:pub:4ECB5004-B2C9-4467-9760-B4F11199DCF8

A redescription of deep-channel ghost knifefish, *Sternarchogiton preto* (Gymnotiformes: Apteronotidae), with assignment to a new genus

Correspondence:
Maxwell J. Bernt
mjbernt@gmail.com

Maxwell J. Bernt[1], Aaron H. Fronk[2], Kory M. Evans[3] and James S. Albert[2]

From a study of morphological and molecular datasets we determine that a species originally described as *Sternarchogiton preto* does not form a monophyletic group with the other valid species of *Sternarchogiton* including the type species, *S. nattereri*. Previously-published phylogenetic analyses indicate that this species is sister to a diverse clade comprised of six described apteronotid genera. We therefore place it into a new genus diagnosed by the presence of three cranial fontanels, first and second infraorbital bones independent (not fused), the absence of an ascending process on the endopterygoid, and dark brown to black pigments over the body surface and fins membranes. We additionally provide a redescription of this enigmatic species with an emphasis on its osteology, and provide the first documentation of secondary sexual dimorphism in this species.

Keywords: Amazonia, Neotropics, Sexual dimorphism, Systematics, Taxonomy.

Submitted November 13, 2019
Accepted February 2, 2020 by William Crampton
Published April 20, 2020

Online version ISSN 1982-0224
Print version ISSN 1679-6225

Neotrop. Ichthyol.
vol. 18, no. 1, Maringá 2020
Epub, Apr 17, 2020

1 Department of Ichthyology, Division of Vertebrate Zoology, American Museum of Natural History, Central Park West at 79th Street, 10024-5192 New York, NY, USA. mjbernt@gmail.com

2 Department of Biology, University of Louisiana at Lafayette, P.O. Box 43602, 70504 Lafayette, LA, USA. (AHF) C00226417@louisiana.edu; (JSA) jalbert@louisiana.edu

3 Department of Ecology and Evolutionary Biology, Brown University, RI 02912 Providence, RI, USA. kxe9300@gmail.com

Através de um estudo com dados morfológicos e moleculares, nós propomos que a espécie originalmente descrita como *Sternarchogiton preto* não forma um grupo monofilético com outras espécies válidas de *Sternarchogiton* incluindo a espécie-tipo, *S. nattereri*. Análises filogenéticas anteriormente publicadas indicam que essa espécie é irmã de um clado diverso contendo seis gêneros descritos de Apteronotidae. Nós então a alocamos em um novo gênero diagnosticado pela presença de três fontanelas craniais, primeiro e segundo ossos infraorbitais independentes (não fusionados), ausência de um processo ascendente do endopterigoide e pigmentação marrom-escura à negra sobre a superfície do corpo e membranas das nadadeiras. Adicionalmente, nós realizamos a redescrição dessa enigmática espécie com ênfase na sua osteologia, e fazemos o primeiro registro de dimorfismo sexual secundário nessa espécie.

Palavras-chave: Amazônia, Dimorfismo Sexual, Neotrópico, Sistemática, Taxonomia.

INTRODUCTION

Sternarchogiton is a genus of weakly electric knifefishes in the family Apteronotidae (the ghost knifefishes) established by Eigenmann in Eigenmann, Ward (1905). The genus was initially proposed in order to recognize two species [*S. nattereri* (Steindachner, 1868) and what is now *Adontosternarchus sachsi* (Peters, 1877)] as distinct from other apteronotids on the basis of a shared reduction in oral dentition. Since the establishment of *Sternarchogiton*, the generic diagnosis has been modified several times with the inclusion of new species or reassignment of existing taxa (Eigenmann, Allen, 1942; Mago-Leccia, 1994; Albert, Campos-da-Paz, 1998; Albert, 2001; Santana, Crampton, 2007). The diagnosis provided in Albert (2001) listed five characters: 1) ventral margin of descending maxillary blade with a sharp angle about two thirds distance to its tip, 2) fourth hypobranchial with medial bridge (here, following Hilton *et al*., 2007, we interpret this bone to be the second hypobranchial), 3) posttemporal not fused with supracleithrum, 4) third postcleithrum not ossified, and 5) descending blades of anal-fin pterygiophores broad distally.

A modified diagnosis was proposed by Santana, Crampton (2007) with a revision of the genus and the description of two new species, *S. labiatus* and *S. preto*. This revision diagnosed the genus by the following five characters: 1) descending blade of maxilla broad, with anterior shelf, 2) ventral margin of descending maxilla bone angled, 3) mandibular canal ossicles dumbbell-shaped, 4) one or two postcleithrae ossified independently, and 5) descending blades of anal-fin pterygiophores broad.

The change in diagnosis was made in order to accommodate the two new species, but also *Sternarchogiton porcinum* Eigenmann, Allen 1942, which was not analyzed in Albert, Campos-da-Paz (1998) or Albert (2001). This expanded diagnosis is problematic, however, because the two maxillary characters are relative. To use the terms “broad” and “angled” with no additional modifiers, illustrations, or comparisons has little diagnostic

value. Notably, *S. preto* and *S. porcinum* both have maxillae that are similar in shape to those of some other apteronotid genera, so there is no clear description of characters of the maxilla that can be used to unite the four species placed in *Sternarchogiton*. Additionally, the characters "mandibular canal ossicles dumbbell-shaped" and "descending blades of anal-fin pterygiophores broad" (characters 91 and 199 in Albert, 2001) are both shared by several other apteronotid groups. In short, species assigned to *Sternarchogiton* are not grouped on the basis of unique shared-derived characters.

A notable feature of apteronotids that has troubled taxonomists is the substantial disparity of characters associated with skull shape and dentition both within and between species. A prominent example is *Sternarchogiton nattereri* in which sexually mature males develop greatly enlarged, protruding teeth, making them appear so different from juveniles and females that they were initially placed in a separate genus (Myers, 1936; Cox-Fernandes *et al*., 2009). Similarly, the long-snouted males of *Parapteronotus hasemani* (Ellis, 1913) were first recognized as a distinct species from the more common short-snouted phenotype (Eigenmann, Allen, 1942; Cox-Fernandes *et al*., 2002). Due to the conserved post-cranial morphology of all Gymnotiformes, osteological characters of the head have been a major source of characters used in morphological systematic analyses. Albert (2001) suggested a close relationship between *Adontosternarchus* Ellis, 1912, *Porotergus* Ellis, 1912, and *Sternarchogiton* based primarily on the osteological characters underlying their similar head and jaw shapes (see Clade AK). However, recent phylogenetic analyses of molecular data place all of these genera into separate lineages (Tagliacollo *et al*., 2016, fig. 2a; Bernt *et al*., 2019). Indeed, long and short-snouted phenotypes are intermixed across the phylogeny, indicating high evolutionary lability in these traits (Albert, Crampton, 2009). As discussed in Bernt *et al*. (2018), this extensive homoplasy necessitates a critical reexamination of apteronotid taxonomy in light of molecular data.

Although the phylogenetic relationships among apteronotids are not completely resolved, several recent analyses have not found *Sternarchogiton* to be monophyletic. Tagliacollo *et al*. (2016) found *S. porcinum* sister to *Compsaraia* Albert, 2001, and these two species as sister to *S. nattereri* and *S. preto*. In contrast, Smith *et al*. (2016), using one nuclear and two mitochondrial loci, placed *S. porcinum* sister to *S. nattereri*, but with *S. preto* sister to all other members of the Navajini. Janzen (2016), using a 9-locus dataset also found *S. preto* sister to all other Navajini, but placed *S. porcinum* sister to *S. nattereri* and *S. labiatus*. Bernt *et al*. (2019), using seven loci recovered the same relationships. Recent examination of the voucher specimen of *S. preto* used in Tagliacollo *et al*. (2016) revealed that this specimen was actually *S. nattereri* or a closely-related undescribed species. Based on these phylogenetic data, we establish a new genus to accommodate *S. preto*, for which there are no known congeners, thereby restricting *Sternarchogiton* to *S. labiatus*, *S. nattereri*, *S. porcinum*, and *S. zuanoni* Santana, Vari, 2010.

MATERIAL AND METHODS

Specimens collected for this study in Brazil and Venezuela were taken using shrimp trawls with a 3 m mouth, 5 m length and 1.5 cm cod-end mesh. Trawls were fished during the day in depths of 2–15 m, generally following the methods of Lopez-Rojas *et*

al. (1984). Specimens collected in the vicinity of Iquitos, Peru were taken using standard methods of local ornamental fish collectors. A large (60 m x 20 m with 8 mm mesh) purse seine was pulled between two motorized canoes at night over depths ranging from 2–10 m.

Morphometric data were taken from 20 specimens using the 25 linear measurements described in Bernt *et al*. (2018). Meristic counts include the anal, caudal, and pectoral-fin rays, precaudal vertebrae, and scales above the lateral line at midbody.

Specimens were cleared and double stained following Taylor, Van Dyke (1985) and microdissection methods followed Weitzman (1974). Osteological illustrations were made from cleared and stained specimens using an Olympus SZX12 microscope equipped with a camera lucida (Olympus SZX-DA). Line drawings were digitally rendered using Adobe Illustrator and edited in Adobe Photoshop. Two specimens were scanned using computed tomography (CT) at the Karel F. Liem BioImaging Center (Friday Harbor Laboratories, University of Washington) using a Bruker (Billerica, MA) SkyScan at a resolution of 28.2 µm. Scans were reconstructed as .bmp image stacks using the Bruker NRecon software. CT data were visualized, segmented, and rendered in Amira (FEI). Anatomical nomenclature follows Mago-Leccia (1978), Fink, Fink (1981), Albert (2001), and Hilton *et al.* (2007).

Material examined are arranged alphabetically by species, country, state, museum, and then number. Following the museum catalog number, we list number of specimens, number of specimens cleared and stained (CS), computed tomography (CT), type status (HT = holotype, PT = paratype), size range of total length in mm, summary of locality, and geographic coordinates. Institutional abbreviations follow Sabaj (2016).

RESULTS

Tenebrosternarchus, new genus

urn:lsid:zoobank.org:act:9205B11E-8A0F-461D-9B43-E309AFC4B204

(Figs. 1–11; Tab. 1)

Type species. *Sternarchogiton preto* Santana, Crampton, 2007, by monotypy.

Diagnosis. *Tenebrosternarchus* is diagnosed from all other apteronotid genera by the following unique combination of four characters: three cranial fontanels present (*vs.* two in other apteronotids), bones 1 and 2 of the infraorbital laterosensory canal present as independently ossified tubes (*vs.* fused into a single bony element), ascending process of endopterygoid absent (*vs.* present), and brown to purplish-black pigment present over the dorsum, sides and fins (*vs.* absent or restricted to dorsum and distal fin margins). For field identification, this genus may be reliably distinguished from all other members of the Navajini by the combination of uniform dark coloration, the presence of five or more teeth on the premaxilla at all life stages, and gape not exceeding a vertical with eye.

Etymology. *Tenebro* from the Latin *tenebrae* meaning darkness in reference to the black pigmentation of this genus, and the Greek *sternarchus* (*sternon* and *archos*), a common generic suffix applied to apteronotids referring to the anterior position of the anus common to all Gymnotiformes.

Tenebrosternarchus preto (Santana, Crampton, 2007), new comb.

Sternarchogiton preto de Santana, Crampton, 2007: fig. 5 table 1 (original description). —Crampton, 2007: 287, 291, 317, table 11.1, 11.2. —Crampton, 2011: 178, table 10.2. —Crampton, Cella-Ribeiro, 2013: 282–283 (photograph). —Silva *et al*., 2014: 638–645, fig. 2. —Tagliacollo *et al*., 2016: 30, fig. 6 (misidentification). —Smith *et al*., 2016: 306–309, fig. 2. —Ferraris, Vari, de Santana, 2017: 12. — Bernt *et al*., 2018: 466, 471, 474–477, table 2. — Bernt *et al*., 2019: 299–302, figs. 3, 4, 6. —Evans *et al*., 2019: 424–425, figs. 2, 3.

Sternarchogiton porcinum Cox-Fernandes, 1995: 32–33, figs. 2–38, 2–39. —Crampton, 1996: fig. 6.1. —Crampton, 1998a: 817, 821, 830, 832, tables 3, 4, 5, 6. —Crampton, 1998b: 315, table 2.

Diagnosis. As for genus.

External morphology. Body shape and pigmentation illustrated in Fig. 1. Summary of morphometric data and meristics shown in Tab. 1. Largest recorded size 330 mm TL. Body elongate and laterally compressed. Body depth greater than head depth. Forehead convex, sloped at approximately 45° in most specimens. Gape extending to or beyond vertical with posterior nares, but not reaching vertical with eye. Mouth subterminal. Eye diameter small, less than 10% head length, covered by thin layer of skin. Scales on body large and rhomboid forming 3–5 rows above lateral line at midbody. Scales absent on entire middorsum and over nape above lateral line to 5th lateral-line pore. Fleshy midsagittal electroreceptive organ originating on posterior third of dorsum. Nasal capsule closer to eye than to snout tip. Anterior nares tubular.

Neurocranium. Neurocranium illustrated in Figs. 2 and 3. Paired frontals convex in lateral profile. Three cranial fontanelles present. Most apteronotid species have only two fontanelles with frontals merging at anterior margin of rear fontanel. In *Tenebrosternarchus*, however, posterior regions of frontals are fused on sagittal midline at margin with parietals, forming a broad isthmus dividing rear fontanel into two smaller openings, one between parietals at their anterior margin and the other at about the posterior third of the frontals. In some specimens, isthmus between frontals appears incompletely merged, with small openings appearing along suture. Mesethmoid decurved in lateral view and forked posteriorly, underlying nasals and bordering anterior fontanelle. Ventral ethmoid robust with wing-like processes extending posterolaterally to contact lateral ethmoid cartilage. Lateral ethmoid thin, slightly broader at ventral articular surface and angled obliquely to neurocranial axis. Orbitosphenoid contacting frontals dorsally, parasphenoid ventrally, and pterosphenoid posteriorly. Together, sphenoid bones form a prominent lateral fenestra. Margin of articulation between orbitosphenoid and pterosphenoid protruding ventrally into anterior third of this fenestra. Forming largest

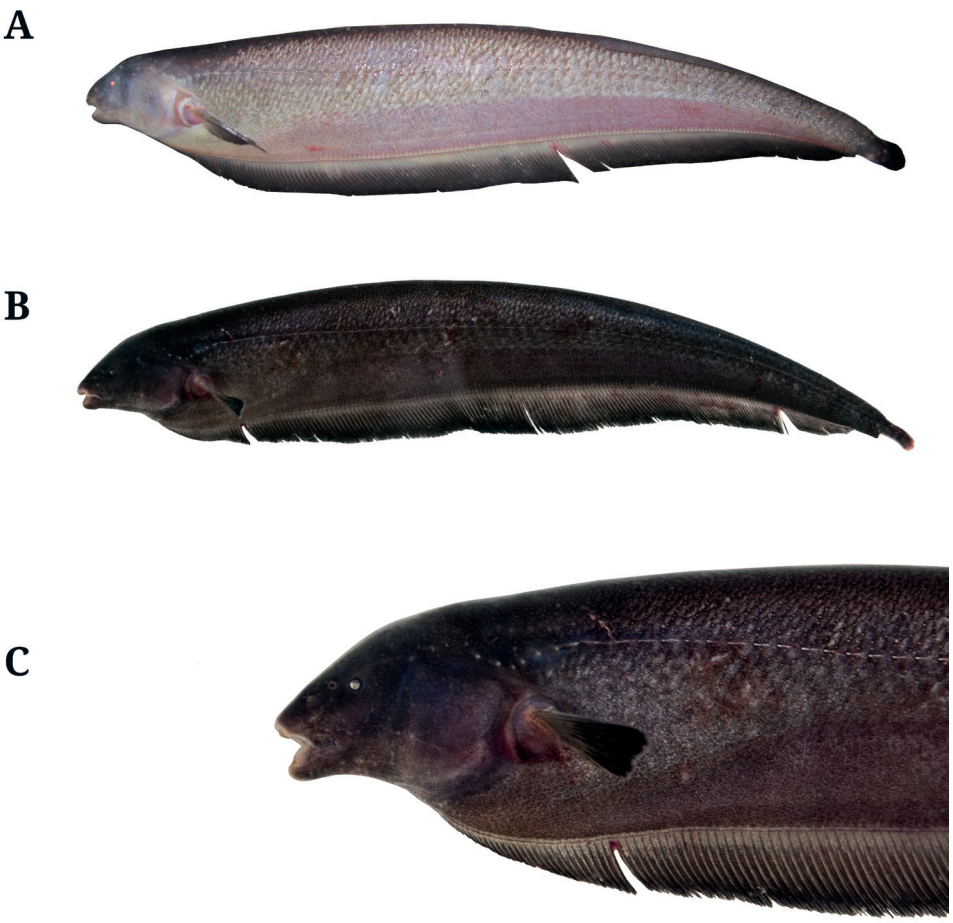

FIGURE 1 | Lateral view of live *Tenebrosternarchus preto*. **A.** MUSM 54656 (243 mm TL) from the río Amazonas at Iquitos, Peru; **B.** ANSP 207797 (232 mm TL) from the rio Negro downstream from Barcelos, Brazil; and **C.** Detail of the head of ANSP 207797 (232 mm TL).

element of skull floor, parasphenoid contacts prootics posteriorly with long and narrow posterior process overlapping with most of basioccipital. Anteriorly, parasphenoid bifurcates into broad processes tapering to sharp points contacting cartilage of ventral ethmoid. Overlying these processes, vomer narrows posteriorly and broadens anteriorly at contact with ventral ethmoid.

Braincase composed of basioccipital, supraoccipital; and paired parietals, epiocciptals, exoccipitals, prootics, pterotics, and sphenotics. Pterotics support horizontal semicircular canals (visible ventrally, Fig. 3B) and form lateral margin of widest region of skull. Prootic and exoccipital with prominent foraminae. Basioccipital approximately rectangular in ventral view, with deep medial groove and circular patch of cartilage at its posterior base. Sphenotics form prominent lateral processes at anterodorsal margin with frontals, nearly reaching width of pterotics. Supraoccipital crest reaching or slightly exceeding dorsal margin of parietals.

Suspensorium and oral jaws. Suspensorium and oral jaws illustrated in Figs. 2 and 4. Opercle with slightly concave dorsal margin. This bone very weakly ossified

with highly reticular structure (see Fig. 2), becoming more laminar at distal margins. Interopercle laminar, but weakly ossified, remaining mostly transparent ventrally after alizarin staining. Subopercle crescent-shaped and similarly thin and transparent distally after staining. Preopercle with vertically-oriented laterosensory canal tube fused to lateral surface and a narrow anteroventral process articulating with quadrate. Hyomandibula oriented about 120° to long axis of skull, with posterolateral ridge contacting dorsal half of preopercular anterior margin. Dorsal articulating head of hyomandibula about twice width of distal end and rounded at point of articulation with sphenotic. Prominent foramen at medial hyomandibular base associated with cranial nerves (V, VII, and lateral line nerves). Symplectic triangular, oblique to hyomandibula and separated by thick, obliquely-angled band of cartilage. Metapterygoid triangular with dorsal and ventral sides about equal in length. Endopterygoid edentulous, lacking ascending process, with blunt posterodorsal process. Endopterygoid broadly overlaps with metapterygoid and quadrate (visible medially). Autopalatine cartilage extending from anterior tip of endopterygoid and abruptly angled laterally, then ventrally to contact articular surface of maxilla.

Mandible comprised of dentary, anguloarticular, retroarticular, Meckel's cartilage and coronomeckelian. Dentary slightly longer than deep with triangular coronoid process and narrow ventral process overlapping with anguloarticular laterally. Anterior ¾ of dentary bearing 13–16 conical teeth arranged in a single row and angled medially (except in some sexually mature males). Anguloarticular forked anteriorly. Dorsal process short, overlapping with dentary laterally. Ventral process long and triangular, broadly overlapping with dentary medially. Retroarticular short and rectangular, without anterior process, contacting only anguloarticular. Meckel's cartilage visible on medial surface of mandible at center of dentary and anguloarticular. Coronomeckelian bone narrow and triangular, contacting dorsal surface of Meckel's cartilage.

Maxilla and premaxilla illustrated in Fig. 5. Maxilla with rounded anteroventral shelf, lacking free anterodorsal hook. Articular process rounded and angled posteriorly. Descending blade of maxilla thin and sharply pointed. Blade extending slightly below horizontal axis of maxillary shelf. Premaxilla broadest anteriorly and narrowing posteriorly. Five to nine large conical teeth present on premaxilla arranged in two uneven rows (but see discussion of sexual dimorphism).

Hyoid arch and branchial basket. Ventral hyoid arch of *Tenebrosternarchus* (illustrated in Fig. 6) notably similar to that of *Apteronotus bonapartii* (see Hilton, Cox-Fernandes, 2017, figs. 6a–b) and *Melanosternarchus* Bernt, Crampton, Orfinger, Albert, 2018 (see Bernt *et al*., 2018, fig. 8). Complex cartilaginous margin between ceratohyals. Posterior ceratohyal rounded at posterior margin with entire anterior surface articulating with anterior ceratohyal. Anterior ceratohyal narrow at posterior margin, broadening anteriorly at margin with dorsal and ventral hypohyals. Dorsal hypohyal articulating with superior surface of ventral hypohyal together forming a pyramidal shape. Ventral hypohyal triangular with point directed anteromedially, with all sides of approximately equal length. Urohyal with medial ridge, lacking posterior blade. Ventral surface with only a very short medial eminence. Four branchiostegal rays. Branchiostegal 1 and 2 slender and filamentous. Third branchiostegal crescent-shaped. Fourth branchiostegal with pointed anterior process, weakly ossified along middle-ventral margin.

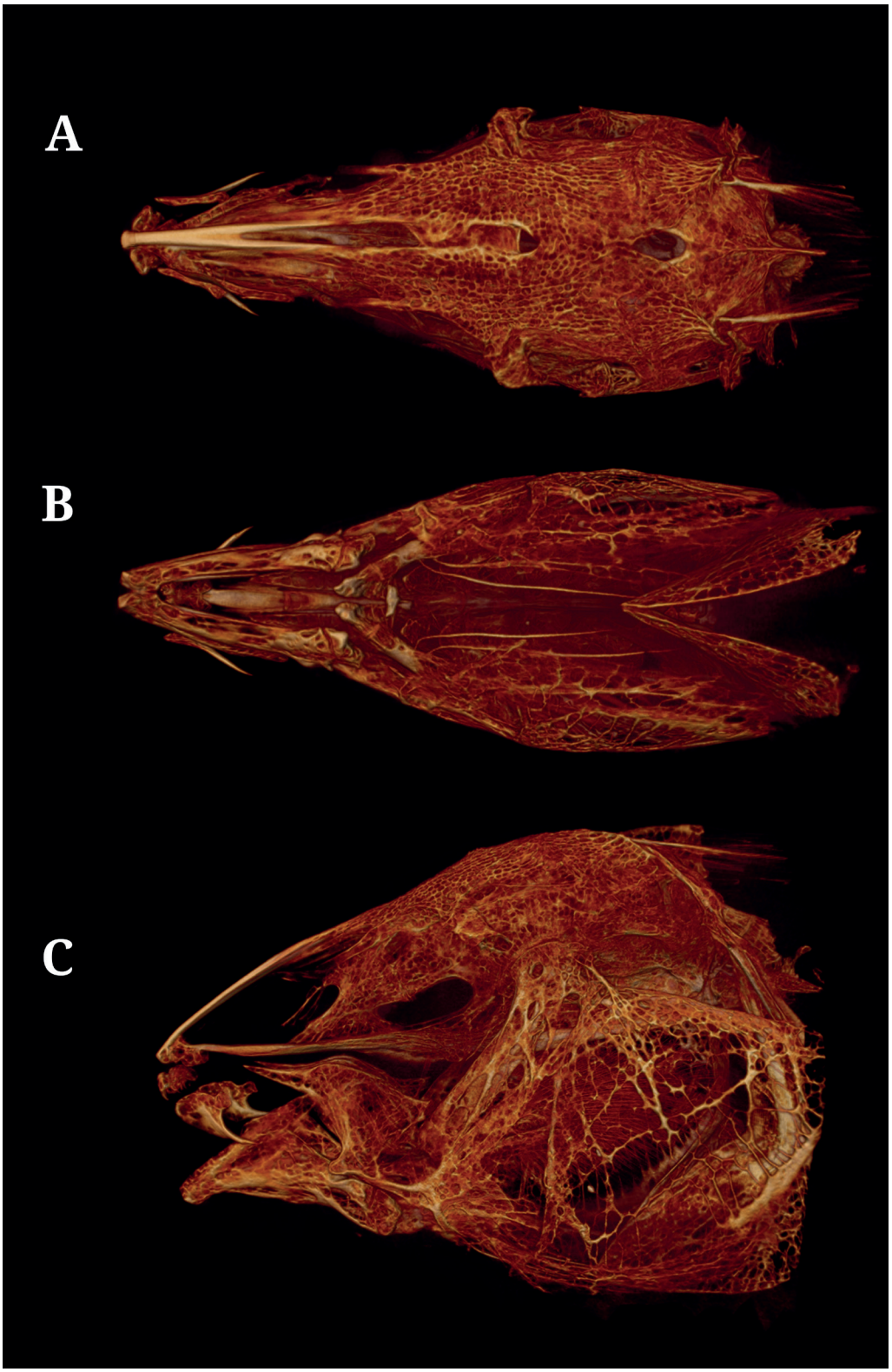

FIGURE 2 | CT scan reconstructions of *Tenebrosternarchus preto*, MUSM 59447 (male) 264 mm TL in dorsal **A.**, ventral **B.**, and lateral **C.** views.

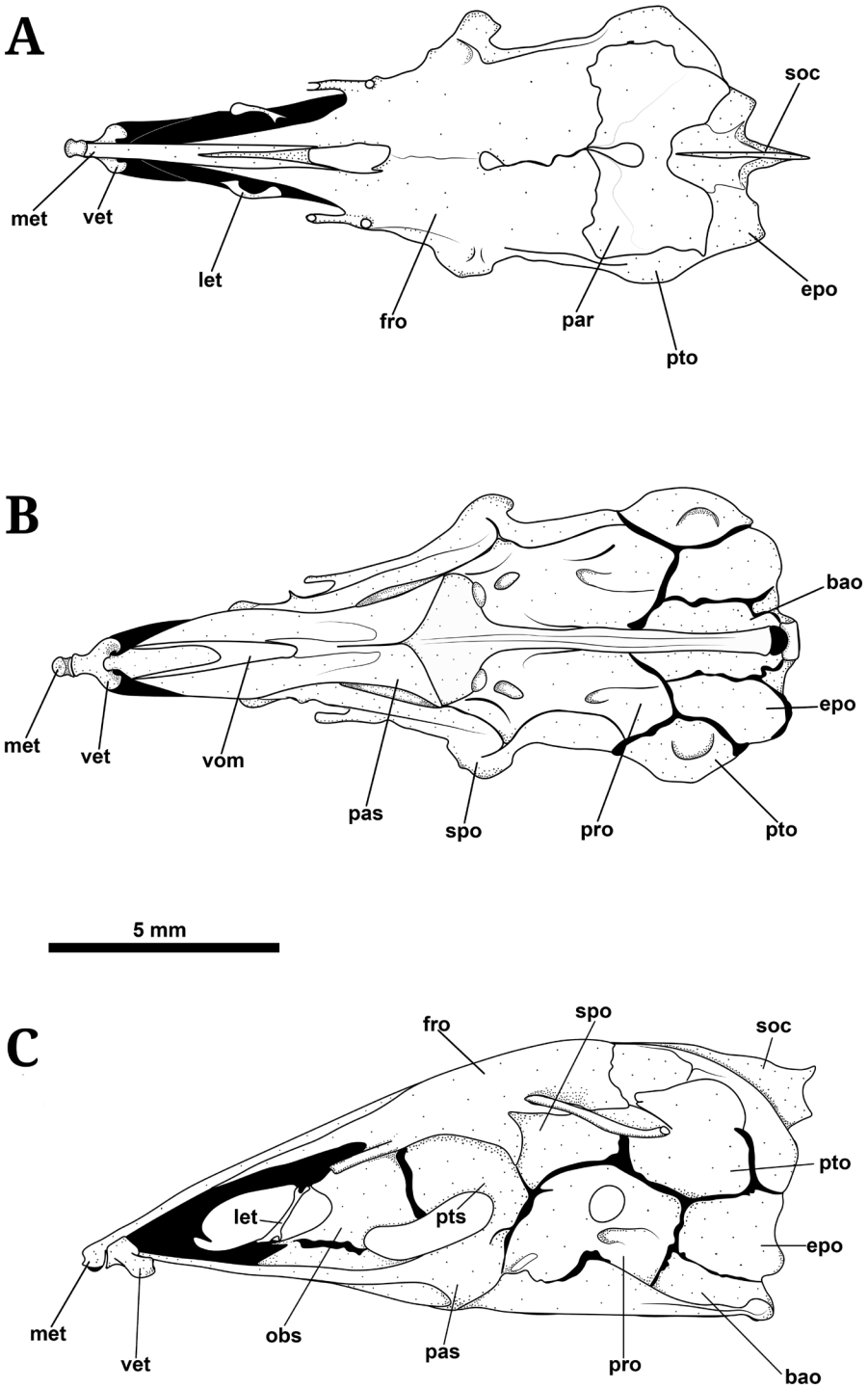

FIGURE 3 | Illustrations of the neurocranium of *Tenebrosternarchus preto* MUSM 54617 (198 mm TL) in dorsal **A.**, ventral **B.**, and lateral **C.** views. Cartilage shown in black. Abbreviations: **bao**, basioccipital; **epo**, epioccipital; **fro**, frontal; **let**, lateral ethmoid; met, mesethmoid; **obs**, orbitosphenoid; **par**, parietal; **pas**, parasphenoid; **pro**, prootic; **pto**, pterotic; **pts**, pterosphenoid; **soc**, supraoccipital; **spo**, sphenotic; **vet**, ventral ethmoid; **vom**, vomer.

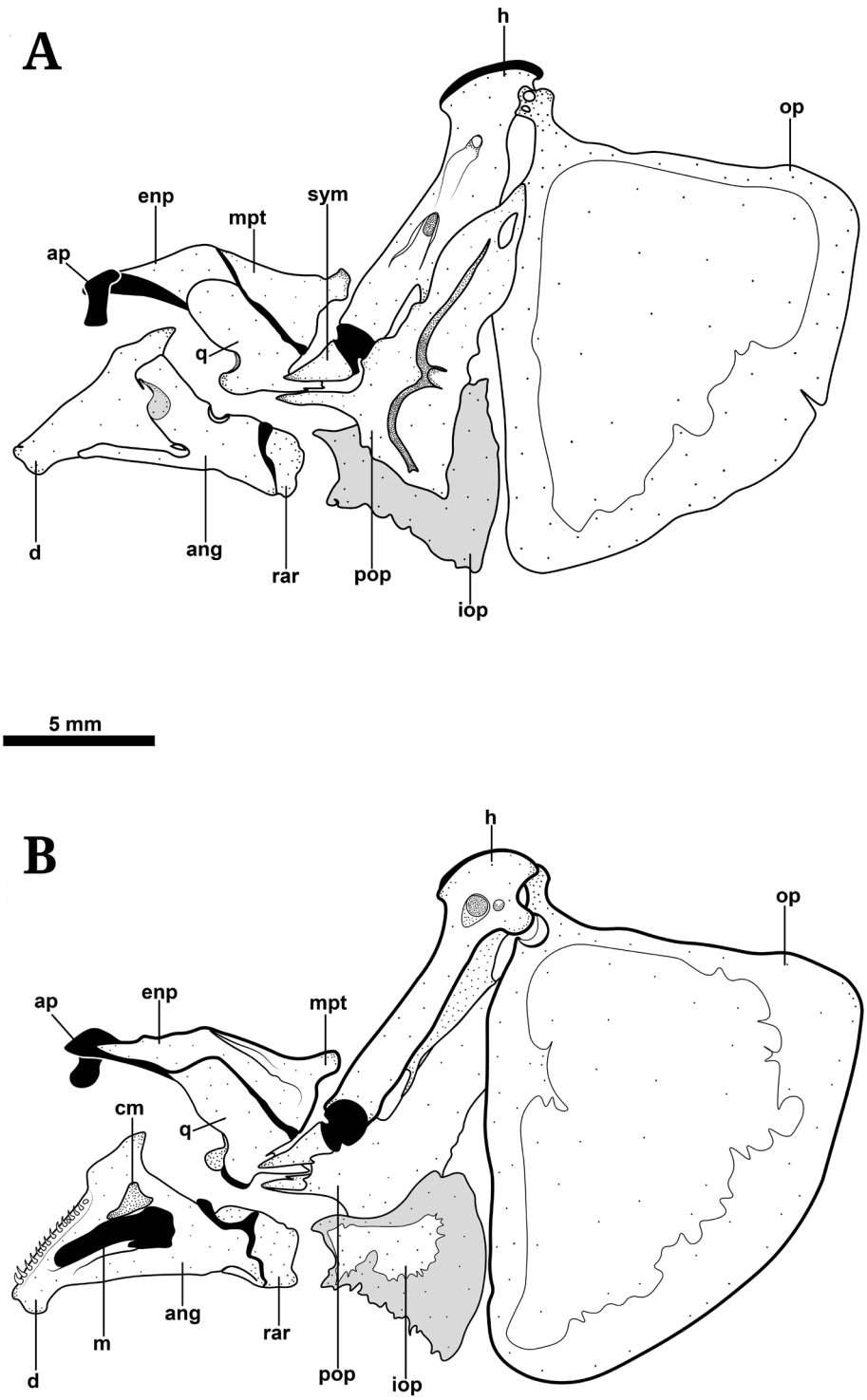

FIGURE 4 | Suspensorium, opercular series, and lower jaw of *Tenebrosternarchus preto*, MUSM 54617 (198 mm TL) in **A.** lateral and **B.** medial view (image reflected). Thin, unstained hard tissue associated with opercular bones shown in light gray. Abbreviations: **ang**, anguloarticular; **ap**, autopalatine cartilage; **cm**, coronomeckelian; **d**, dentary; **enp**, endopterygoid; **h**, hyomandibula; **iop**, interopercle; **m**, Meckel's cartilage; **mpt**, metapterygoid; **op**, opercle; **pop**, preopercle; **q**, quadrate; **rar**, retroarticular; **sym**, symplectic.

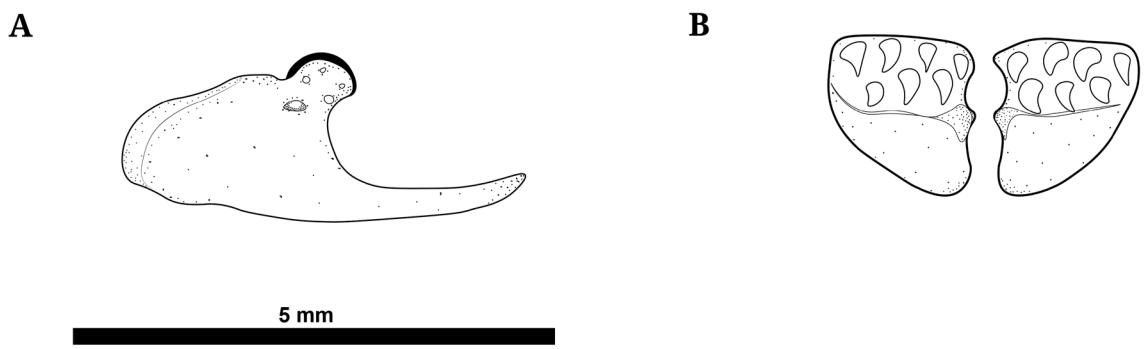

FIGURE 5 | Maxilla of *Tenebrosternarchus preto*. **A.** MUSM 54617 (198 mm TL) in lateral view; and **B.** the paired premaxillae of the same specimen in ventral view.

Ventral branchial basket illustrated in Fig. 7A. We follow Hilton *et al*. (2007) in interpreting anteriormost element of ventral branchial skeleton as a fused basihyal and first basibranchial. This structure broadened anteriorly with cartilaginous tip and narrow posteriorly with thin dorsal ridge. Second basibranchial hourglass-shaped, convex at anterior and posterior articular surfaces. Third basibranchial ossified, broader anteriorly than posteriorly. Basibranchials 4 and 5 unossified, present as cartilaginous rods. First hypobranchials roughly conical and cartilaginous posteriorly. Second hypobranchials contacting medially beneath second basibranchial. Third hypobranchials contacting medially posterior to third basibranchial. Ceratobranchials 1 and 2 roughly rectangular, with cartilaginous cap at dorsal tip. Ceratobranchial 3 narrow at point of articulation with hypobranchials, with medial hook and short, ventral process. Ceratobranchial 4 very slender medially with medial process at about midlength of bone. Six gill rakers associated with each of first four ceratobranchial bones. Fifth ceratobranchials contacting medially around a small circular element of cartilage. Posteromedial surface of ceratobranchial 5 bearing 8–10 conical teeth.

Dorsal elements of branchial basket illustrated in Fig. 7B. Epibranchials 1 and 2 approximately rectangular, associated with few (1–2) or no gill rakers. Epibranchial 3 with short anteromedial process contacting infrapharyngobranchial 3. Epibranchial 4 Y-shaped, forked posteriorly, contacting epibranchial 5. Epibranchial 5 entirely cartilaginous, tapering posteriorly to a sharp point. Infrapharyngobranchials 1 and 2 broad posteriorly with thick cartilaginous articular surface contacting epibranchial laterally and next infrapharyngobranchial medially. Third infrapharyngobranchial rod shaped and entirely cartilaginous. Upper pharyngobranchial tooth plate positioned over articulation between infrapharyngobranchial 3 and epibranchial 4. Upper tooth plate substantially smaller than lower plate and weakly-ossified, bearing 6 teeth.

Cranial laterosensory system. Cephalic laterosensory canals illustrated in Fig. 8. Three nasal canal-bones present as small ossified tubes. Most posterior nasal canal (superior to posterior naris) more than twice length of other two. Anterior half of this canal visible as a groove, or incompletely formed tube. Elongate supraorbital canal fused with frontal bone. Antorbital bone present as small tubular ossification immediately

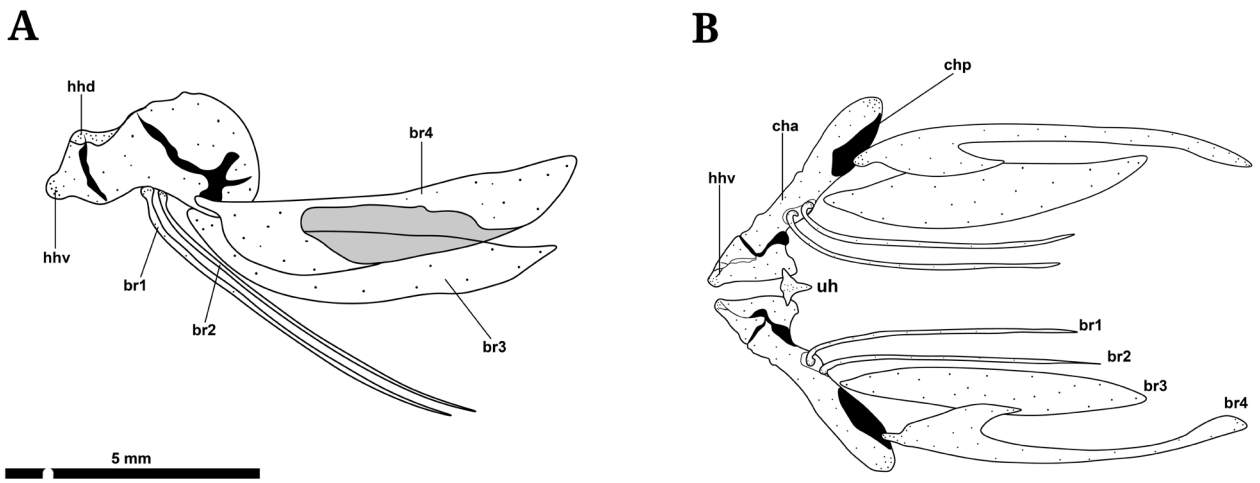

FIGURE 6 | Elements of the ventral hyoid arch of *Tenebrosternarchus preto* in **A.** lateral and **B.** ventral view MUSM 54617 (198 mm TL). Anterior facing left. Abbreviations: **br**, branchiostegal; **cha**, anterior ceratohyal; **chp**, posterior ceratohyal; **hhd**, dorsal hypohyal; **hhv**, ventral hypohyal; **uh**, urohyal.

below posterior nares and anterior to eye. Infraorbital bones 1, 2, and 3 present as independently ossified tubes below anterior naris. Fourth infraorbital below antorbital. Infraorbitals 5 and 6 more than twice length of infraorbitals 1–4, positioned posterior to eye. Parietal canal not ossified in specimens observed. Horizontally-oriented otic canal forming longest element of cephalic laterosensory system immediately anterior to a short postotic canal. Supratemporal canal straight, vertically-oriented forming a right angle with postotic. Posterior-most element of cranial laterosensory system fused to posttemporal, ventroposterior to postotic and supratemporal canals. Five mandibular canals present as short, sharply-curved ossicles. Anterior four mandibular canals ventrolateral to dentary, posterior mandibular canal lateral to base of preopercle.

Weberian apparatus and vertebral column. Posterior to the skull, first four vertebrae and associated elements comprise the Weberian apparatus. Fifth vertebra articulating with first rib. First rib robust and with greatly expanded parapophysis, contacting enlarged fourth parapophysis forming ventrally-angled concavity that contacts dorsolateral surface of anterior region of swim bladder. First neural spine distally broadened. Fifteen to 17 precaudal vertebrae including those associated with Weberian apparatus, extending to but not including vertebra articulating with anterior-displaced hemal spine. Anterior-displaced hemal spine long and saber-shaped, forming posterior margin of body cavity, its dorsal articular surface contacted by parapophysis of one or two vertebrae (see Fig. 9). Two to three posterior-displaced hemal spines articulating with base of hemal spines of first two caudal vertebrae, sometimes including vertebra articulating with anterior-displaced hemal spine.

Pectoral girdle. Pectoral girdle illustrated in Fig. 10. Two weakly-ossified, rectangular postcleithrae present. Dorsal extension of cleithrum with groove, closely

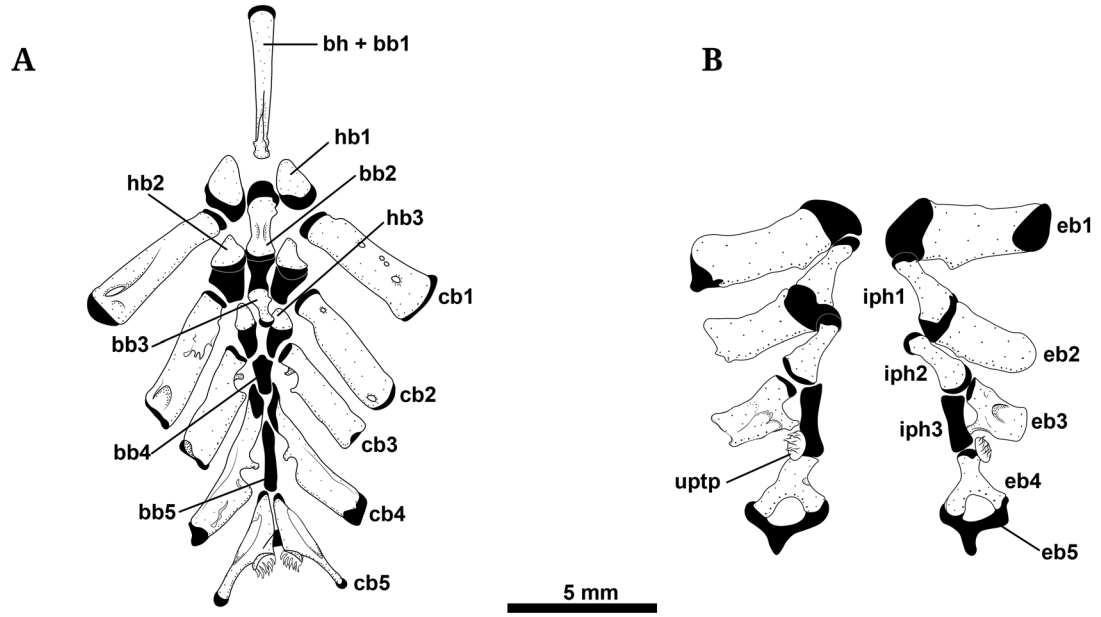

FIGURE 7 | Gill arches of *Tenebrosternarchus preto*, MUSM 54617 (254 mm TL) Ventral arches **A.** shown in dorsal view and dorsal arches **B.** in ventral view. Abbreviations: **bb**, basibranchial; bh, basihyal, **cb**, ceratobranchial; **eb**, epibranchial; **hb**, hypobranchial; **iph**, infrapharyngobranchial; **uptp**, upper pharyngeal toothplate.

associated with supracleithrum. Supracleithrum with notch-like articular surface for ventrally-broadened posttemporal. Anterodorsally angled laterosensory canal fused to posttemporal near point of contact with supracleithrum. Scapula broadest dorsally along contact with cleithrum, angling anteriorly to contact coracoid. Coracoid with dorsally expanded process contacting cleithrum near point of dorsal flexion and thin anterior process contacting ventral margin of cleithrum. Four irregularly-shaped proximal radials. Propterygium with broad cartilaginous base. Fourteen to 17 pectoral-fin rays. First ray about half length of remaining rays.

Fins, rays, and pterygiophores. Anal fin with 152–204 rays (mode = 193, n = 20). Anal-fin pterygiophores longer than hemal spines along most of body length. Anal-fin pterygiophores broadened ventrally into symmetrical vanes above their articulation with distal radials. Caudal fin size and shape variable with 12–23 (mode = 14) rays. Caudal fin frequently absent, damaged, or regenerated (as in most apteronotids), presumably due to electroreceptive predators. Number of rays higher (and fin size larger) in many specimens with regenerated caudal fins. Ray counts for all fins include both branched and unbranched rays.

Color pattern. In life, *Tenebrosternarchus* ranges from slate gray to deep black in color. Pigment is darkest over top of head, middorsum, and nape. These regions devoid of scales are finely dotted with pale-colored tuberous electroreceptor organs. Dorsal organ paler in color than skin of other parts of dorsum, usually dark gray. Sides of body above anal-fin pterygiophores variable in coloration, scales darker at their bases. Region

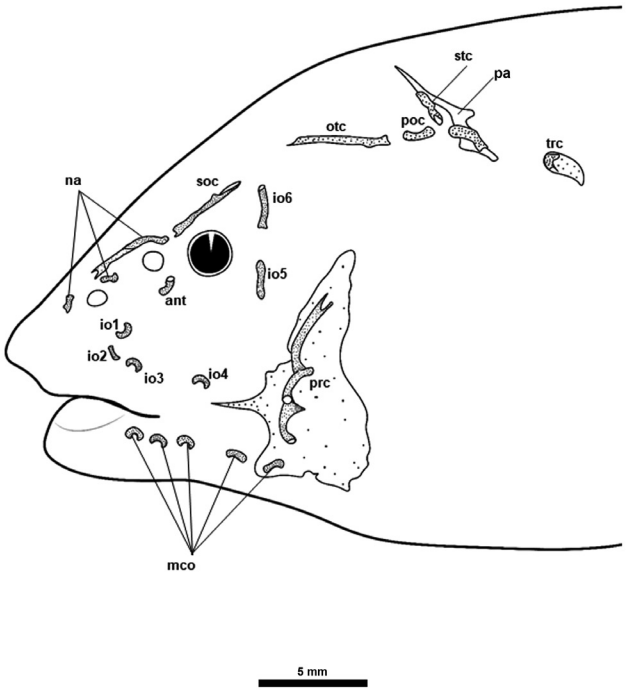

FIGURE 8 | Cephalic lateral-line bones of *Tenebrosternarchus preto*, MUSM 54617 (198 mm TL). Abbreviations: **ant**, antorbital; **io**, infraorbital; **na**, nasal; **otc**, otic canal; **mco**, mandibular canal ossicles; **pa**, parietal canal; **poc**, postotic canal; **prc**, preopercular canal; **soc**, supraorbital canal; **stc**, supratemporal canal; **trc**, trunk canal.

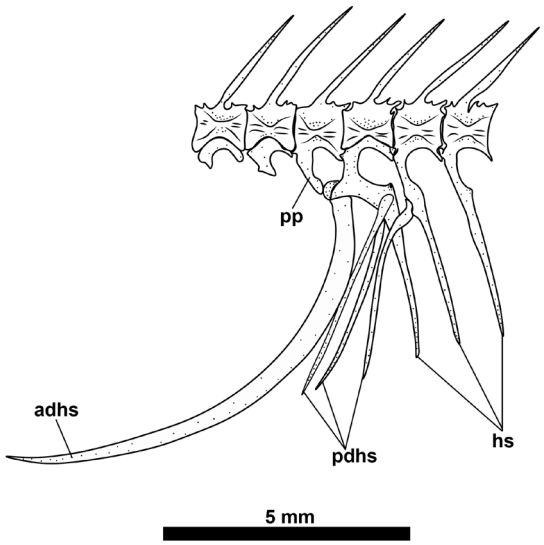

FIGURE 9 |Displaced hemal spine configuration of *Tenebrosternarchus preto*, MUSM 54617 (198 mm TL). Abbreviations: **adhs**, anterior displaced hemal spine; **hs**, hemal spine; **pp**, parapophysis; **pdhs**, posterior displaced hemal spine.

overlying pterygiophores have a deep purplish-red to lighter pink coloration. Anal fin dark brown to black, except in a narrow hyaline band along proximal margin. Pectoral and caudal fins uniformly dark brown to black. Opercular region with rosy coloration due to underlying gill lamellae. Fleshy region of upper lower jaw and margin of upper lip a pale cream color. Like Santana, Crampton (2007) we also notice that color varies with habitat. In particular we found that specimens from blackwater rivers (*e.g.,* the rio Negro) were darker due to a visibly higher density of black chromatophores over body, while specimens taken from turbid whitewaters (especially the río Apure) were lightest in coloration with more gray and pink hues (see Figs 1 and 11). Coloration in ethanol similar to that in life, but with reddish to pink colors fading to brown and beige, and pale cream colors fading to dull yellow.

Sexual dimorphism. Three specimens of *Tenebrosternarchus* were found to exhibit a more laterally protuberant snout with a less steeply sloping forehead and a longer gape than the majority of samples (see Fig. 11). Upon inspection of the gonads, it was found that all of these hypertrophied specimens were male. Notably these male specimens were all near or exceeding 300 mm in length. Several males under 250 mm TL did not exhibit distinct cranial morphology and could be sexed only by the presence of testes. The two largest male specimens exhibited increased dentition with over 20 teeth on each premaxilla and two to three rows of dentary teeth. Both also showed scars

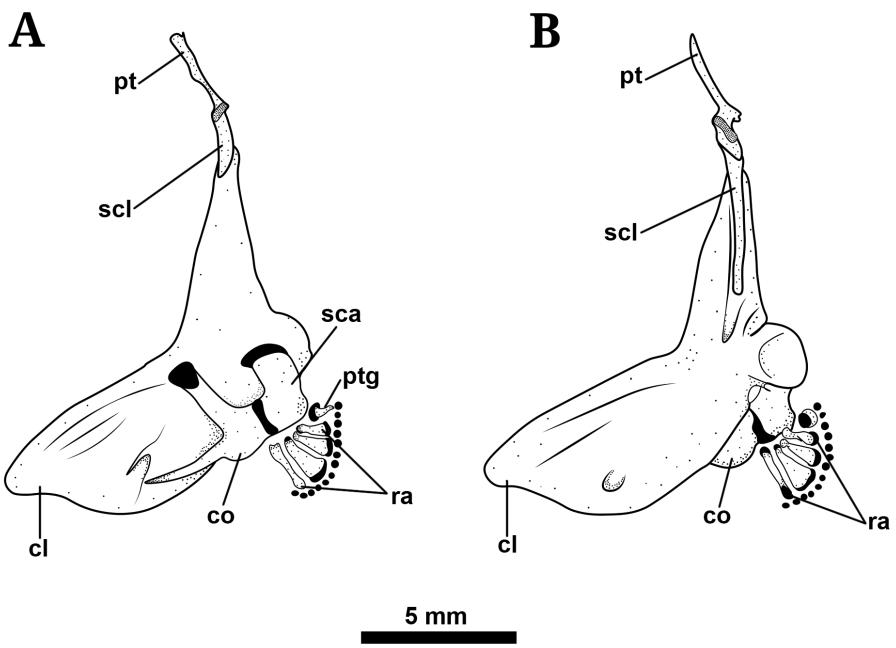

FIGURE 10 | Pectoral girdle of *Tenebrosternarchus preto*, MUSM 54617 (198 mm TL) in lateral **A.**, and medial **B.** views. Abbreviations: **cl**, cleithrum; **co**, coracoid; **pt**, posttemporal; **ptg**, propterygium; **ra**, radial; **sca**, scapula; **scl**, supracleithrum.

and lacerations around the head and nape. This condition is commonly observed in male *Sternarchogiton nattereri* with enlarged external teeth and are presumed to be the result of male-male combat (Cox-Fernandes *et al*., 2009). The largest specimen of *T. preto* examined (330 mm TL) was a female that did not exhibit any distinct cranial morphology or increased dentition. The largest male specimen (MUSM 59463) was distinct enough from other *T. preto* that it was thought possible that it was a different species entirely. Genetic analysis of tissue taken from this specimen, however, showed it to be nested within Amazonian specimens of *T. preto* (specimen IQ17039).

Ecology. Little is presently known about the ecology of *Tenebrosternarchus*. Typically among ghost knifefishes, species inhabiting deep river channels (*sensu* Crampton, 2007) have greatly reduced pigmentation, often appearing pink or white (*e.g*., *Orthosternarchus* Ellis, 1912, *Sternarchella* Eigenmann, 1905), while those inhabiting smaller streams or marginal habitats of larger rivers have much darker coloration (*e.g*., *Apteronotus* Lacepède, 1800, *Platyurosternarchus* Mago-Leccia, 1994). Interestingly, *T. preto*, with its dark coloration, appears to be an obligate channel-dweller, and does not appear to frequent shallower waters more than other members of the Navajini. This genus does seem to have a habitat preference for low-conductivity blackwater rivers as a majority of specimens we examined were collected from the rio Negro and the río Nanay (both blackwater rivers). This preference for blackwater does not appear to be as strict as that of *Melanosternarchus* (see Bernt *et al*., 2018), as specimens of *T. preto* are also collected from whitewater channels (*e.g*., the Amazon, Apure, and Madeira rivers). Specimens are also known from near the mouths of clearwater rivers (Tapajós and Xingu), but

TABLE 1 | Summary of morphometric and meristic data for *Tenebrosternarchus preto*, N = 20 from ANSP 200470, MUSM 59463, MUSM 59447, MUSM 54617, and MUSM 54656.

Character	Mean	Range
Total length (TL)	—	87–330
Length to end of anal fin (LEA)	—	77–290
Anal fin base (AFB)	—	68–260
Caudal appendage length (CL)	—	9–70
Tail depth (TD)	—	1.1–11.8
Head length (HL)	—	10.2–39
Length to origin of dorsal organ (LOD)	—	55–187
Body depth/LOD	0.23	0.18–0.35
Prepectoral length/LOD	0.24	0.22–0.28
Preanal length/LOD	0.16	0.13–0.25
Snout-anus length/HL	0.53	0.41–0.70
Pectoral fin length/HL	0.75	0.51–1.2
Head depth at opercle/HL	0.94	0.75–1.1
Head depth at eye/HL	0.56	0.49–0.65
Head width/HL	0.48	0.42–0.53
Snout length/HL	0.35	0.30–0.42
Postorbital/HL	0.7	0.56–1.0
Gape length/HL	0.25	0.16–0.34
Eye diameter/Postorbital length (PO)	0.1	0.06–0.13
Posterior naris-snout/PO	0.4	0.25–0.52
Posterior naris-eye/PO	0.09	0.05–0.18
Internarial distance/PO	0.15	0.1–0.23
Interocular width/PO	0.36	0.19–0.43
Branchial opening/PO	0.41	0.22–0.53
Body width/PO	0.61	0.36–0.78
	Mode	**Range**
Anal-fin rays	193	152–204
Pectoral-fin rays	16	14–17
Caudal-fin rays	14	12–23

they are not known to be more abundant in these rivers than in whitewaters. Nearly all specimens from whitewater rivers have regenerated caudal fins (a common condition among apteronotids), while undamaged tails are more common from blackwater with about 70% of specimens showing signs of regeneration.

Tenebrosternarchus is typically found among aggregations of other channel knifefishes, especially *Rhabdolichops* Eigenmann, Allen, 1942, *Sternarchella*, *Orthosternarchus* Ellis, 1912, and *Sternarchorhamphus* Eigenmann, 1905. It tends to be relatively uncommon in trawl samples, but was found to be locally abundant on the río Nanay in the vicinity of Iquitos, Peru during low water (June–August). Notably, specimens collected at this time and place were found to be substantially larger in average size (250–300 mm) than those from other collections. Examination of gut contents of several specimens from this habitat revealed that *T. preto* feeds most heavily on chironomid larvae, though coleopteran and ceratopogonid larvae were also present. These larvae were found to be mixed with sand

FIGURE 11 | Heads of male *Tenebrosternarchus preto* **A.** ANSP 198373 (302 mm TL) from the río Apure at San Fernando de Apure, Venezuela **B.** MUSM 59463 (291 mm) and **C.** MUSM 59447 (320 mm TL) both from the río Nanay at Iquitos, Peru.

and detritus, suggesting that *T. preto* is a primarily a benthic forager. Crampton (2007) also reports that this species feeds on freshwater sponges of the genus *Drulia*.

Distribution. The collection localities of samples analyzed in this study are summarized in Fig. 12. Our examined material of *Tenebrosternarchus* ranges from the western Amazon at Iquitos, Peru to the mouth of the rio Xingu in Pará, Brazil, the rio Negro, from Manaus to Barcelos, and the Orinoco Basin in Venezuela, from the río Apure at San Fernando de Apure to near the mouth of the río Orinoco in Delta Amacuro. Crampton, Cella-Ribeiro (2013) also report this species from the Madeira drainage above the extensive system of cataracts beginning at Porto Velho.

Phylogenetic relationships. The molecular phylogeny of Bernt *et al*. (2019) placed *Tenebrosternarchus* sister to all other species in the Navajini, which form a clade comprised of the *Apteronotus bonapartii* group, *Compsaraia*, *Melanosternarchus*, *Pariosternarchus* Albert, Crampton, 2006, *Porotergus*, *Sternarchella*, and *Sternarchogiton*. This phylogeny included eight specimens of *T. preto*. Five of these were from the western Amazon at Iquitos, one was from the lower Amazon at Santarem, and two were from the Orinoco drainage (río Apure). The latter two samples are sister to the remaining six, however, the branch length separating them is comparable to intraspecific branchlengths throughout the family. Additionally, morphometric and meristic data do not suggest the presence of multiple allopatric species within the sample we analyzed. The relationship of

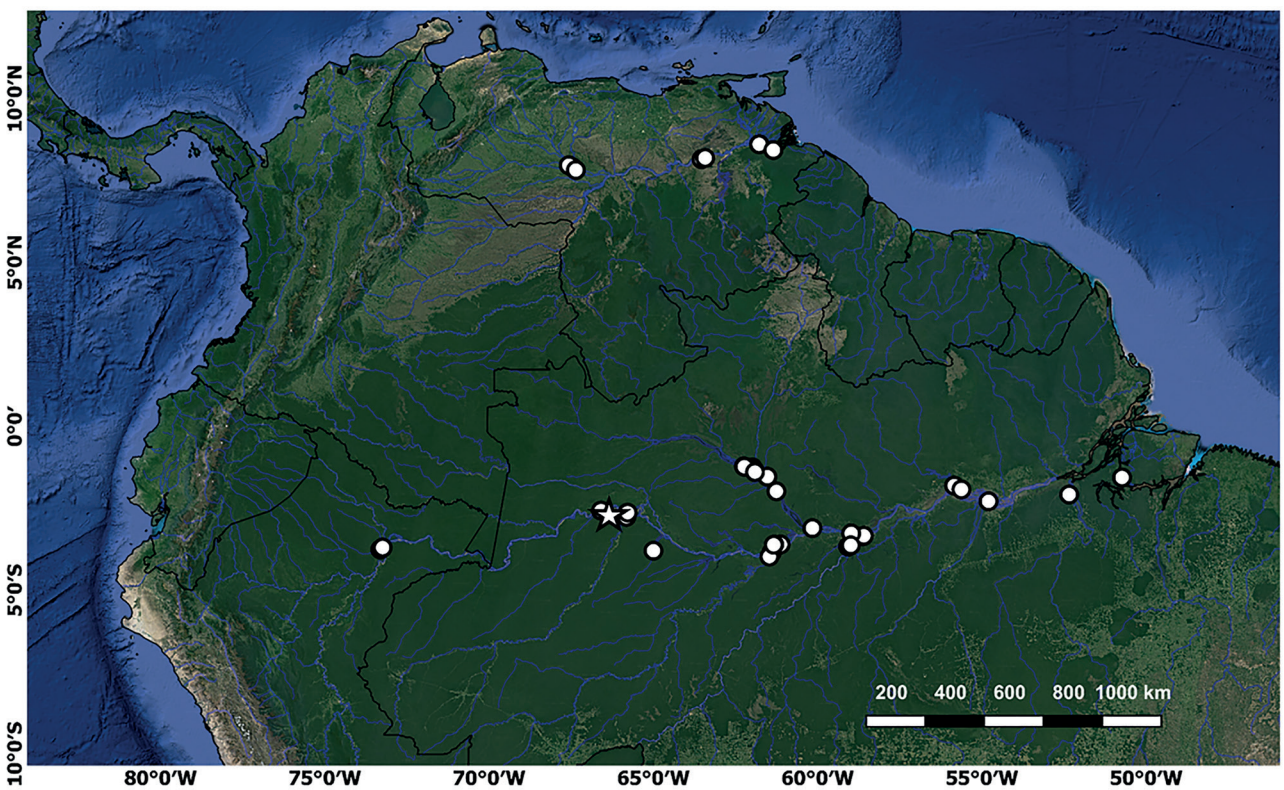

FIGURE 12 | Collection localities of *Tenebrosternarchus preto*, star indicating type locality. Some points indicate multiple collections or lots from proximate locations.

Tenebrosternarchus to other genera is well supported with a bootstrap value of 98% and a posterior probability of 1.

Material examined: Brazil: **Amazonas**: AMNH 221206, 5, rio Negro between Tarumã and Tarumã Mirim, 7 Nov 1997, C. Cox Fernandes, J. Lundberg. ANSP 189211, 1, rio Negro, 10 km downstream from Carvoeiro, 1°22'8"S 61°54'22"W, 9 Dec 1993, J. Lundberg *et al*. ANSP 189221, 1, rio Juruá downriver of Pauapixuna, upriver of Vitoria, 2°41'8"S 65° 48'29"W, 9 Nov 1993, J. Lundberg *et al*. ANSP 189222, 1, rio Juruá downstream of Humaitá, upstream of Pauapixuna, 2°45'19"S 65°49'15"W, 9 Nov 1993, J. Lundberg *et al*. ANSP 189223, 1, rio Negro, 34.3 km downriver of Novo Caioe, 4.4 km upriver of São Francisco de Assis, 1°58'37" S61°15'21"W, 5 Dec 1993, J. Lundberg *et al*. ANSP 189224, 1, rio Negro, 62 km downriver of Vila Guajara, 47.2 km upriver of Moura, 1°14'51"S 61° 58'52"W, 9 Dec 1993, J. Lundberg *et al*. ANSP 189225, 2, rio Juruá 17.3 km downriver of Pauapixuna, 15.7 km upriver of Tamanicoa, 2°37'36.9"S 65°47'01.8"W, 7 Nov 1993, O. Oyakawa, J. Lundberg, *et al*. ANSP 199741, 1, rio Tefé, in floating macrophytes (Projeto Mamirauá), 1994, W. Crampton. ANSP 195681, 14, rio Negro, 4.3 km downstream of Carvoeiro, 37.0 km upstream of Moura, 1°20'26"S 61°55'19"W, 9 Dec 1993, J. Lundberg *et al*. ANSP 195682, 2, rio Solimões below mouth of rio Purus, 3°35'51.4"S 61°07'40.8"W, 31 July 1996, M. Toledo-Piza, J. Lundberg *et al*. ANSP 195683, 1, rio Amazonas downriver of mouth of rio Madeira, upriver of Itacoatiara, 3°20'45.8"S 58°37'50.3"W, 8 August 1996, M. Toledo-Piza, J. Lundberg *et al*. ANSP 195684, 1, rio Amazonas, 159 km downstream of Manaus, 30 km upstream of Itacoatiara, 3°19'60"S 58°35'44"W, 10 Aug 1996, C. Cox Fernandes, J. Lundberg *et al*. ANSP 195686, 1, rio Negro downstream of Vila Guajara and upstream of Carvoeiro, 1°13'31.5"S 62°13'57.5"W, 10 Dec, 1993, J. Lundberg *et al*. ANSP 195688, 3, rio Negro above rio Jufari, 34.3 km downriver of Vila Guajara, 1°12'52"S 62°14'41"W, 10 Dec 1993, J. Friel, J. Lundberg *et al*. ANSP 195689, 10, rio Negro, 1.9 km above confluence with rio Branco, 9.3 km downstream of Carvoeiro, 34.8 km upstream of Moura, 1°22'21"S 61°54'32"W, 9 Dec 1993, J. Lundberg *et al*. ANSP 195690, 9, rio Negro, 26.3 km downriver of Vila Guajara, 35.4 km upriver of Carvoeiro, 1°13'33"S 62°13'54"W, 10 Dec 1993, M. Garcia, J. Lundberg *et al*. ANSP 195691, 1, rio Solimões, 27.8 km downriver of Foz do Jutaí, 6.9 km upriver of Ponta Grossa, 2°33'52"S 66°35'37"W, 12 Nov 1993, J. Lundberg *et al*. ANSP 195692, 1, rio Negro, 10.6 km downriver of Leprosario, 14.8 km upriver of Manaus, 3°6'0"S 60°9'33"W, 10 Oct 1994, J. Lundberg *et al*. ANSP 195693, 1, rio Negro, 12.6 km downriver of Moura, 20.7 km upriver of São Francisco, 1°31'45"S 61°31'52"W, 7 Dec 1993, M. Garcia, J. Lundberg *et al*. ANSP 195694, 1, rio Purus upstream from confluence with rio Solimões, downstream of town of Beruri, 3°49'53"S 61°24'7"W, 26 Jul 1996, A. Zanata, J. Lundberg *et al*. ANSP 195695, 1, rio Purus, 4 km upriver of São Tomé, 8 km downriver of Beruri, 3°50'35"S 61°23'45"W, 26 Jul 1996, F. Langeani, J. Lundberg *et al*. ANSP 195696, 1, rio Madeira, 25.9 km downriver of Nova Olinda do Norte, 0.7 km upriver of Rosarinho, 3°39'50"S 59°4'15"W, 16 Oct 1996, F. Langeani, J. Lundberg *et al*. ANSP 195697, 1, rio Solimões, below mouth of rio Purus, 3°36'1.2"S 61°19'20.3"W, 28 Jul 1996, A. Zanata, J. Lundberg *et al*. ANSP 195698, 2, rio Purus above confluence with rio Solimões, 10 nautical miles downriver of Surará, 8 nautical miles upriver of Beruri, 3°58'02.4"S 61°28'01.6"W, 27 Jul 1996, J. Lundberg *et al*. ANSP 195699, 2, rio

Amazonas, upstream of Itacoatiara, 3°15'33"S 58°58'42"W, 5 Aug 1996, A. Zanata, J. Lundberg *et al.* ANSP 195700, 1, rio Madeira, upriver of Urucurituba, 3°37'25"S 58°59'33"W, 7 Aug 1996, A. Zanata, J. Lundberg *et al*. ANSP 195702, 1, rio Solimões, 37.2 km downriver of Anori, 3 km upriver of Porto S. Francisco, 3°36'23"S 61°20'11"W. ANSP 207840, 5, 2 CS, rio Demeni, 18 km upstream of confluence with rio Negro, 0°38'28.8"S 62°53'47.5"W, 29 Nov 1993, J. Lundberg *et al*. ANSP 207903 (5), Furo of rio Demeni near mouth of Parana do Camuqual, 0°24'57.6"S 62°53'37.8"W, 12 Aug 2018, M. Bernt, G. Costa Silva, B. Waltz. ANSP 195704, 4, rio Negro, 5.0 km upriver of mouth of rio Branco, 7.9 km downriver of Carvoeiro, 1°23'19.9"S 61°54'29.2"W, 8 Dec 1993, J. Friel, J. Lundberg *et al*. ANSP 207873, 2, rio Araçá immediately upstream from confluence with rio Demini, 0°24'54.4"S 62°56'9.1"W, 11 Aug 2018, M. Bernt, G. Costa Silva, B. Waltz. ANSP 207797, 1, rio Negro at Lagoa do Pato, 1°12'16.5"S 62°23'9.3"W, 6 Aug 218, M. Bernt, G. Costa Silva, B. Waltz. **Pará**: ANSP 195687, 9, rio Amazonas, 9.7 km downstream of Vila Canaã, 10.2 km upstream from Porto S. José, 1°33'22"S 50°44'5"W, 16 Nov 1994, A. Zanata, J. Lundberg *et al*. ANSP 195685, 3, rio Acarai upstream from confluence with rio Xingu, Porto de Moz, 2°4'34"S 52°20'42"W, 10 Nov 1994, A. Zanata, J. Lundberg *et al*. ANSP 195701, 2, rio Trombetas, 3.6 km downriver of Oriximiná, 2.9 km upriver of Fazenda Paraiso, 1°48'7"S 55°50'52"W, 24 Oct 1994, J. Lundberg *et al*. ANSP 195703, 2, rio Amazonas above mouth of rio Trombetas, 13.3 km upriver of Óbidos, 1°55'10.5"S 55°37'26.9"W, 23 Oct 1994, M. Westneat, J. Lundberg *et al*. ANSP 200380, 1, rio Tapajós at mouth, *ca*. 18 km north-northwest of Santarém, 2°16'52.7"S 54°47'59.9"W, 18 Jun 2015, J. Albert, V. Tagliacollo *et al*. **Peru**: **Loreto**: ANSP 200246, 3, río Nanay near confluence with río Amazonas, 3°41'32.9"S 73°14'32.6"W, 18 Aug 2015, K. Evans *et al*. ANSP 200470, 2, río Nanay upstream of Pampachica, 3°44'50.6"S 73°18'45.1"W, 2 Jan 2016, M. Bernt, E. Chota *et al*. ANSP 200551, 3, río Amazonas near mouth of río Nanay, 3°41'32.9"S 73°14'32.6"W, 2 Sep 2016. MUSM 54617, 13, 2 CS, río Nanay upstream from Manacamiri, sandy beach across from small quebrada, 3°44'29.55"S 73°17'3.88"W, 4 Jul 2014, M. Bernt, D. Saldaña *et al.* MUSM 54656, 1, río Amazonas near Iquitos 3°49'11.5"S 73°09'31.2"W, 7 Jul 2014, M. Bernt, D. Saldaña *et al*. MUSM 59447, 8, 2 CS, río Nanay, beach upstream of Pucayacu a Orillas, 3°45.712'S 73°18.901'W, 2 Jan 2017, M. Bernt, R. Cahuaza *et al*. MUSM 59463, 2, río Nanay at Pampachica, 3°45'09.0180"S 73°16'54.6924"W, 5 Jan 2017, M. Bernt, R. Cahuaza *et al*. **Venezuela**: **Apure**: ANSP 198346, 1, río Apure, channels on both sides of small island, *ca*. 12 km downstream of Aeropuerto Las Flecheras, *ca*. 15.5 km east-southeast of Puente María Nieves, San Fernando de Apure, 7°49'04.2"N 67°21'30.6"W, 10 Apr 2015, M. Sabaj, M. Bernt, O.Castillo *et al*. ANSP 198373, 1, río Apure, *ca*. 5 km upstream of mouth of río Portuguesa, 7°57'51.1"N 67°34'36.4"W, 9 Apr 2015, M. Sabaj, M. Bernt, O.Castillo *et al*. ANSP 198391, 1, río Apure, just downstream of Puente María Nieves, San Fernando de Apure, 7°53'55.3"N 67°27'32"W, 8 April 2015, M. Sabaj, M. Bernt, O.Castillo *et al*. **Bolivar**: ANSP 149504, 1, río Orinoco, south side of river at Ciudad Bolivar, 241 nautical mi from sea buoy, 8°9'N 63°32'W, 8 Nov 1979, E. Marsh *et al*. ANSP 199016, 1, río Orinoco, electric power line crossing at narrows below Ciudad Bolivar, 234 nautical miles from sea buoy, station no. 36917, 300 meters from shore, 8°11'06"N 63°25'30"W, 9 Nov 1979, J. Lundberg *et al*. **Delta Amacuro**: AMNH 217738, 1, río Orinoco, from buoy 129.7 to buoy 130.4 at Isla Tres Caños, downstream from El Consejo and Barrancas, 14 Nov

1979, J. Baskin, G. Miller *et al*. ANSP 149529, 3, río Orinoco, downstream from mouth of río Arature, *ca*. km 51. ANSP 199012, 2, río Orinoco just downstream of Isla Portuguesa *ca*.116.5 naut. mi. from sea buoy, 8°36'12"N 61°46'24"W, 24 Feb 1978, J.

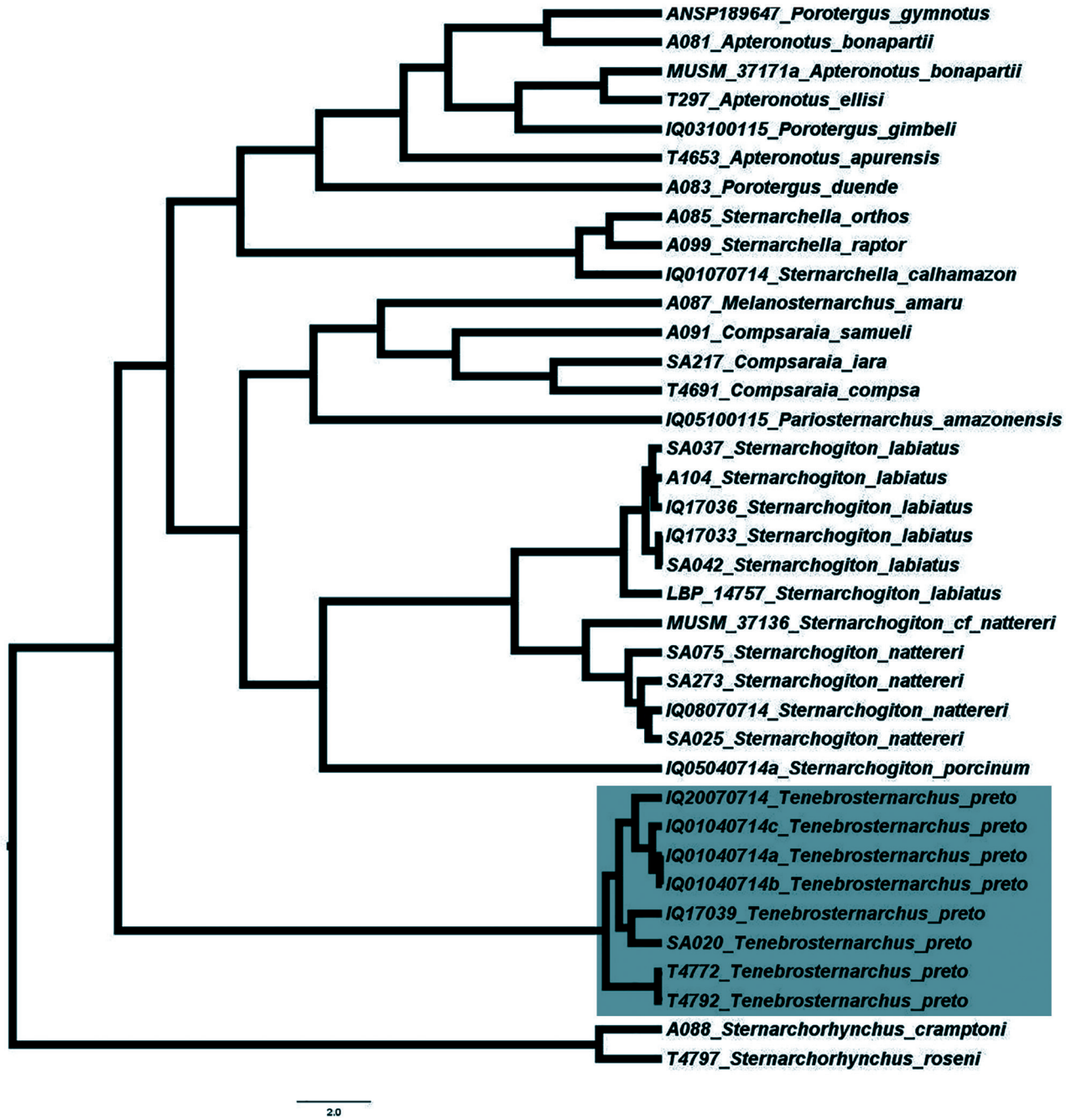

FIGURE 13 | Phylogenetic position of *Tenebrosternarchus* (■) within the Navajini modified from Bernt *et al.*, 2019. Topology is a summary of maximum likelihood and Bayesian analyses of seven concatenated loci from Bernt *et al.* (2019). All nodes shown in this topology have bootstrap support values at or above 85% and posterior probabilities above 0.90.

Lundberg, J. Baskin *et al*. ANSP 199018, 1, río Orinoco, just downstream of Isla Portuguesa, *ca*. 116.5 nautical miles from sea buoy, 8°36'12"N 61°46'54"W, 14 Nov 1979, J. Lundberg *et al*. ANSP 199019, 1, río Orinoco, old shipping channel S of Portuguesa, *ca*. km 117, 20 Feb 1978, J. Lundberg *et al*. ANSP 199248, 1, Small caño (caño "Electrica") and swamp off río Orinoco, near buoy 85.7, on N side of Isla Carosimo, 8°25'36"N 61°20'54"W, 21 Nov 1979, D. Stewart *et al*. ANSP 199006, 1, río Orinoco: near mouth of río Arature, *ca*. km 53, 24 Feb 1978, J. Lundberg, J. Baskin *et al*.

DISCUSSION

Our knowledge of the Apteronotidae is growing rapidly, with the number of valid species more than doubling since Albert's comprehensive revision of Gymnotiformes in 2001. In addition to adding more species, we are also gaining new phylogenetic insights. Several new molecular phylogenies have recently been proposed for Apteronotidae that reveal incongruences between the inferred relationships and the established taxonomy. In particular, Janzen (2016), Smith *et al*. (2016), and Bernt *et al*. (2019) all independently reveal that the genera *Apteronotus*, *Porotergus*, and *Sternarchogiton* are not monophyletic. These genera, therefore, are most likely the result of grouping based on convergent or plesiomorphic characters.

In the case of *Sternarchogiton*, each topology placed *T. preto* sister to the six other genera that make up the Navajini (see Fig. 13). The Navajini is a morphologically diverse group including extremely long-snouted species (*e.g*., *Compsaraia samueli* Albert, Crampton, 2009), species with large, robust teeth (*e.g*., *Sternarchella* spp.), and species with greatly reduced dentition (*e.g*., *Porotergus duende* de Santana, Crampton, 2010, *Melanosternarchus amaru* Bernt, Crampton, Orfinger, Albert, 2018). The distant placement of these species raises the question of how morphologically distinct *Tenebrosternarchus* really is from *Sternarchogiton.* We find several characters to be useful in making this assessment. To begin with, the diagnostic trait of three cranial fontanels (or a divided posterior fontanel) is unique within the Navajini. Notably, this character is apparently not associated with short-snouted phenotypes (*i.e.* brachycephaly) as the other species of short-snouted apteronotids (*e.g*., *Porotergus* and *Adontosternarchus*) and even brachycephalic genera in other families (*e.g*., *Eigenmannia* Jordan, Evermann, 1896 and *Steatogenys* Boulenger, 1898) all have two cranial fontanels. To our current knowledge this character is found only in one other apteronotid species, *Parapteronotus hasemani*, which is not a member of the Navajini and does not bear other appreciable similarities to *Tenebrosternarchus*.

The dark coloration of *Tenebrosternarchus* is also unique within the Navajini. As a clade of predominantly deep-channel specialists, a majority of species in the Navajini have greatly reduced pigment and appear pink or white in life. *Melanosternarchus* and members of the *Apteronotus bonapartii* group tend to have much more brown and black pigment than other members of the Navajini, but neither of these has the uniformity of dark pigment exhibited by *Tenebrosternarchus*. However, as noted in the description, this dark coloration is variable with habitat and therefore does not discretely differentiate *Tenebrosternarchus* from other members of the Navajini. It does, however, differentiate it from *Sternarchogiton*, in which dark pigmentation is limited to the fins of *S. labiatus* and *S. porcinum*.

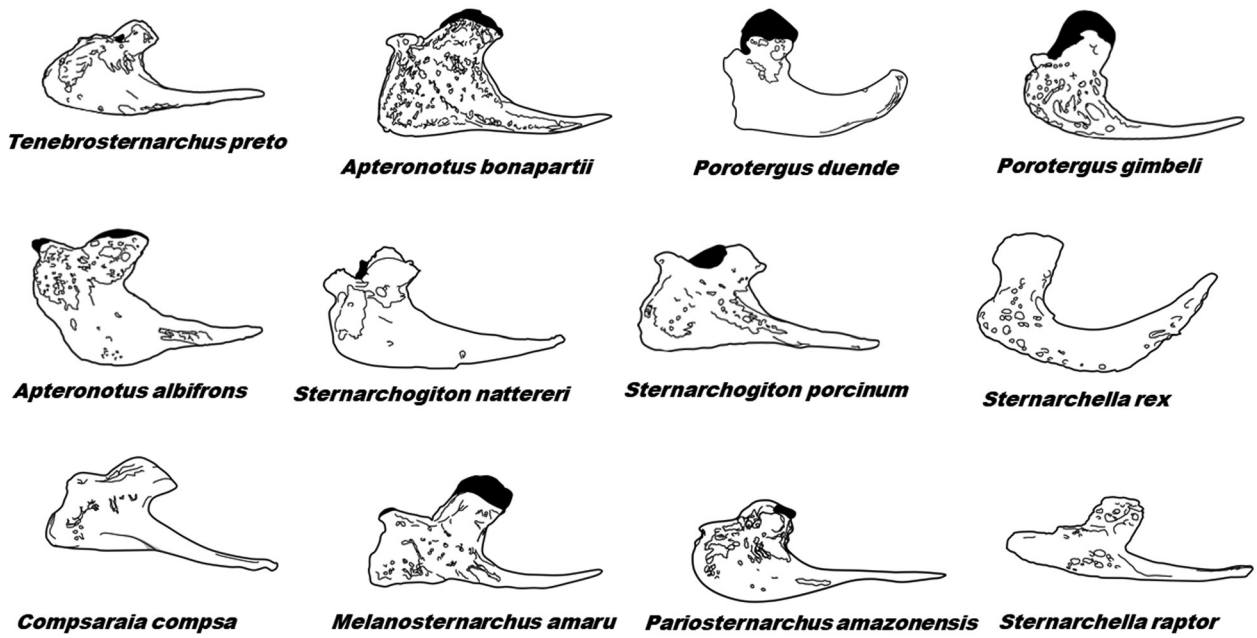

FIGURE 14 | Sample of diversity of maxilla shape in Apteronotidae, emphasizing the Navajini. Maxillae are illustrated in lateral view and are not drawn to scale.

Morphological characters of dentition are problematic in grouping apteronotid taxa due to their substantial differences within and among species (see Bernt, Albert, 2017; Bernt *et al*., 2018). A majority of specimens of *Tenebrosternarchus* have 5–9 teeth on each premaxilla, while a majority of specimens of *Sternarchogiton* have none. However, some mature male *S. nattereri* grow numerous teeth on the premaxilla, while other apparently mature males have none or exhibit intermediate phenotypes (Cox-Fernandes *et al*., 2009). The extent to which the other species of *Sternarchogiton* exhibit sexual dimorphism in dentition is not known, but at least one specimen of *S. porcinum* has been found to have premaxillary teeth (pers. obs.). In general, *Tenebrosternarchus* has more teeth than *Sternarchogiton*, but the variability in this character due to sexual dimorphism limits its value in a diagnosis.

Several other characters of the jaw and suspensorium are of ambiguous use in separating *Tenebrosternarchus* and *Sternarchogiton*. *Tenebrosternarchus* lacks an ascending process of the endopterygoid, a condition shared by *S. labiatus*. However, both *S. porcinum* and *S. nattereri* have this process. The shape of the maxilla was previously used by Santana, Crampton (2007) as a character to diagnose *Sternarchogiton* (then including *T. preto*). However, the character state was poorly described and as Fig. 14 indicates, the maxillae of *Tenebrosternarchus* and *Sternarchogiton* bear no unique similarity to each other when compared to those of other apteronotids. The autopalatine cartilage of *Tenebrosternarchus* has an abrupt lateral curve to contact the maxilla. This condition is closely matched in both *S. labiatus* and *S. nattereri*. It would seem that this character is associated with a foreshortened snout as it is not observed in the longer-snouted *S. porcinum*, but a similar condition is seen in the brachycephalic *Porotergus duende* and some species of *Sternarchella*.

The cephalic laterosensory system has not been extensively studied in Apteronotidae, but it does appear to differ substantially among groups within the Navajini. In *Tenebrosternarchus*, the laterosensory canals are present as narrow, lightly-ossified tubes, a condition common to apteronotids outside the Navajini, but also shared by *Sternarchella*. Additionally, the six infraorbitals of *Tenebrosternarchus* are small, independent canals. These characters contrast sharply with the robust laterosensory canal systems found in *Melanosternarchus*, *Pariosternarchus*, and *Compsaraia*. These genera, along with *Sternarchogiton* and the *Apteronotus bonapartii* group all also have a fused first and second infraorbital unlike *T. preto*. Notably *S. porcinum* has robust mandibular canal ossicles much like those of *Compsaraia*, so in general the entire Navajini B clade (*sensu* Bernt *et al*., 2019) can be distinguished by a more robustly ossified cranial laterosensory system than observed in *Tenebrosternarchus*.

Taken together, these characters support the recognition of *Tenebrosternarchus* as a distinct lineage from the genus *Sternarchogiton,* and that convergence between these clades does not extend substantially beyond their shared brachycephalic phenotype. As apteronotids are highly conserved in post-cranial morphology, the cranium is the most prominent axis of phenotypic diversity. The prevalence of brachycephalic phenotypes across the apteronotid phylogeny is a continual source of taxonomic confusion. Evans *et al*. (2017) recognize a developmental bias toward brachycephaly in Apteronotidae and other Gymnotiformes. While noting that short-snouted phenotypes evolve more frequently across the phylogeny, brachycephalic taxa also exhibit a wider range of trophic phenotypes, from planktivory in *Adontosternarchus* to piscivory in *Sternarchella*. Therefore, while brachycephalic phenotypes are superficially similar, in-depth anatomical studies reveal substantial structural and functional diversity.

In its original description, Santana, Crampton (2007) state that *T. preto* is not sexually dimorphic based on the analysis of 12 mature males and nine mature females, however they do not list the sizes of the specimens that were examined. It is possible that all of their male specimens were too small to exhibit sexual dimorphism. It is also possible that not all males exhibit a distinct terminal phenotype. This has been noted in *Sternarchogiton nattereri* by Cox-Fernandes *et al.* (2009) and in *Compsaraia samueli* (pers. obs.). Among all sexually-dimorphic apteronotids, the extreme male phenotypes are rare in collections and tend to appear only during the high-water season.

We have also recently received photographs from ornamental fish exporters showing fish similar to *T. preto* (see Fig. 15) exhibiting an even greater lengthening of the snout and partially everted teeth on both jaws. This phenotype appears to be an extension of the condition observed in our largest male specimen, suggesting that this species may exhibit a more extreme sexual dimorphism like that of other apteronotid species, but a closer analysis of these strange phenotypes is needed. From our observations we can conclude that *T. preto* is sexually dimorphic in head shape and dentition, but additional specimens are needed in order to provide a more thorough description of the male phenotype and its osteology.

Comparative Material Examined. *Adontosternarchus balaenops:* MUSM 54639, 4, 133–174. *Adontosternarchus devenanzii*: ANSP 198405, 4, 125–169. *Adontosternarchus sachsi*: ANSP 200434, 1, 137. *Apteronotus albifrons*: ANSP 198394, 1, 165. UF 2991, 11, 1 CS, 84–236. *Apteronotus apurensis*: ANSP198350, 67, 1 CS, 181–312. ANSP 198362,

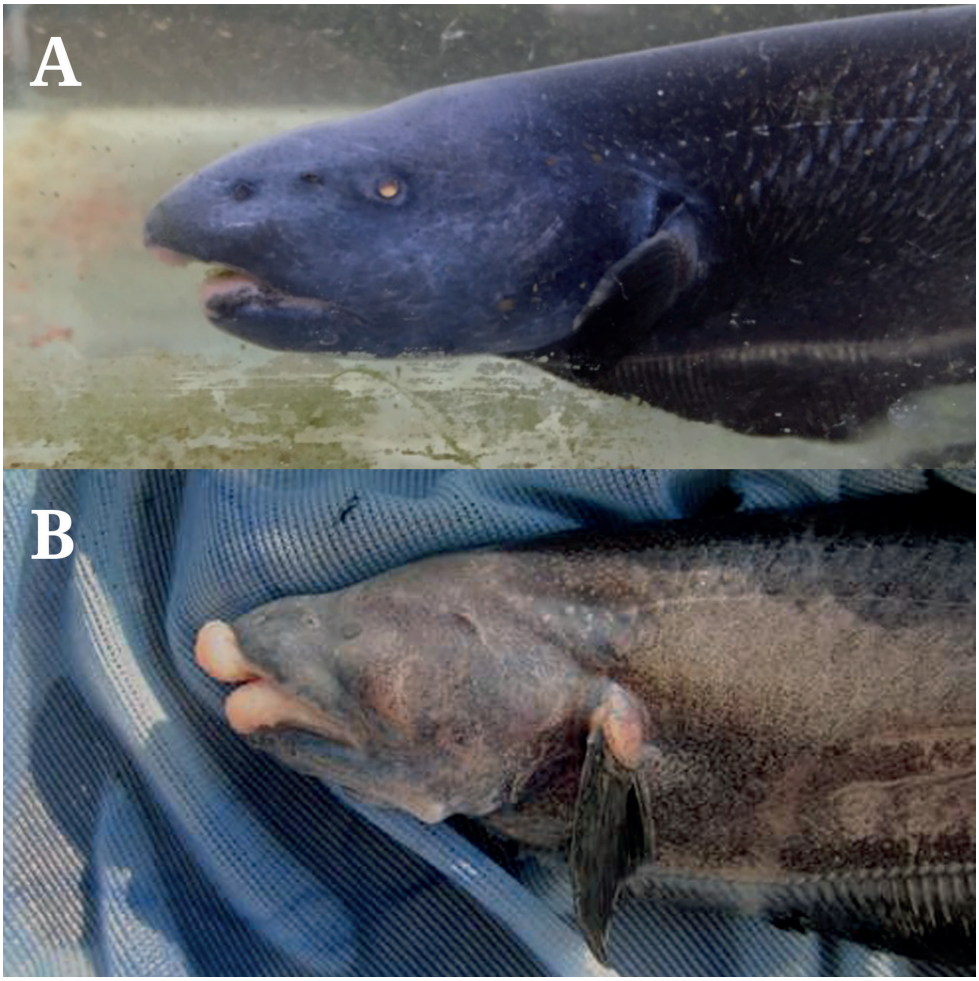

FIGURE 15 | Apteronotids collected by ornamental fish wholesalers tentatively identified as male *Tenebrosternarchus preto* exhibiting hypertrophied jaws and everted teeth. **A.** Specimen locality unknown, photo courtesy of Kazuyuki Muramatsu. **B.** Specimen collected in the vicinity of Iquitos, PE, photo courtesy of Minoru Matsuzaka.

20, 151–297. ANSP 198374, 13, 1 CS, 120–291. FMNH 85499, 31, 56–189. UF 80733, 1 CS, 204. FMNH 100739, 1, 135. ANSP 163037, 2, 159–188. ANSP 149505, 1, 186. *Apteronotus* cf. *baniwa*: UF 33905, 2, 133–136. *Apteronotus bonapartii*: ANSP 192673, 1, 149. ANSP 192684, 1, 155. ANSP 195219, 1, 189, rio Solimões 15.6 km above mouth of rio Jutaí, 13.9 km upriver of Foz do Jutaí, 2°40'29.9"S 66°51'56.7"W. ANSP 195229. ANSP 200445, 5, 1 CS, 109–151. ANSP 200397, 4, 119–137. AUM 23717, 6, 1 CS. UF 23848, 1, 132. UF 23854, 1, 137. FMNH 100618, 1, 113. ANSP 200458, 5, 157–198. ANSP 200499, 5, 142–225. ANSP 182585, 3, 135–172. MNHN 3807, 1, 240. MUSM 54641, 30, 2 CS, 106–207. MUSM 36837, 2, 198–223. MUSM 37171 (2), 123–137. *Apteronotus ellisi*: DZUFMG 57, 4, 2 CS. LBP 4333, 1, 200. *Apteronotus rostratus*: STRI 8653, 2, 149–153. *Compsaraia compsa*: ANSP 163035, 12, 75–202. UMMZ 230828, 20, 164–259. Apure: ANSP 165223 (2), 246–250. ANSP 198399, 1, 257. ANSP 160194, 1 PT, 262. Barinas: FMNH 100737, 5. ANSP 163033, 53, 9 CS, 90–326. ANSP 162671, 2, 239–273. AMNH 217678, 2, 290–303. ANSP 149522, 20, 117–216. ANSP 149514, 2,

255–260. *Compsaraia iara*: Brazil: Amazonas: ANSP 192781, 1 PT, 220. FMNH 128428, 1 PT. MZUSP 56074, 15, PT. ANSP 195554, 9, 137–181. FMNH 115028, 14, 3 CS, 133–216. FMNH 115029, 1, 198. MZUSP 121514, 1 HT. *Compsaraia samueli*: ANSP 185098, 3, 1 CS, 141–162. ANSP 189212, 2, 140–221. FMNH 115060, 12, 180–241. FMNH 115054, 3, 185–197. FMNH 115061, 1, 201. ANSP 197672, 11, 140–204. FMNH 114973, 27, 61–125. FMNH 114945, 13, 109–150. ANSP 182209, 2 PT, 132–188. ANSP 182214, 1 PT, 159. FLMNH 122826, 1, 209. MUSM 54620, 43, 3 CS, 110–181. MUSM 59454, 21, 133–165. MUSM 54638, 10, 68–151. MUSM 37172, 6, 3 CS. MUSM 37150, 1, 259. MUSM 36716, 1, 292. *Megadontognathus cuyuniense*: MCNG 10956, 2 PT, 190–215. *Megadontognathus kaitukaensis*: ANSP 195961, 1, 168. *Melanosternarchus amaru*: ANSP 200451, 1 PT, 262. ANSP 200452, 1, 177. ANSP 200459, 12 PT, 2 CT, 149–231. *Orthosternarchus tamandua*: MUSM 54618, 2, 336–346. *Parapteronotus hasemani*: MUSM 54647, 3, 187–299. MUSM 54688, 1, 297. UF 116563, 3, 1 CS, 102–250. *Pariosternarchus amazonensis*: ANSP 192996, 3, 1 CS, 100–110. MCP 34917, 1 CS, PT. FMNH 128402, 2, 189–192. ANSP 200453, 1, 160. ANSP 200454, 1, 282. *Platyurosternarchus macrostomus*: ANSP 200406, 2, 335–342. MUSM 54680, 4, 2 CS, 251–340. *Porotergus duende*: ANSP 200463, 14, 2 CS, 90–175. ANSP 200483, 6, 67–190. *Porotergus gimbeli*: ANSP 200375, 4, 117–131. MUSM 54677, 4, 1 CS, 120–176. *Porotergus gymnotus:* OS 18509, 1, 171. AUM 28071, 1, 107. FMNH 53575, 1 HT, 65. FMNH 53291, 1 PT, 58. ANSP 189647, 1, 150. *Sternarchella calhamazon*: ANSP 200394, 2, 131–170. *Sternarchella orthos*: ANSP 200429, 3, 126–195. *Sternarchella raptor*: MUSM 54643, 4, 72–104. MUSM 54640, 2, 67–97. UF 116762, 1 CS, 205. *Sternarchella schotti*: ANSP 200500, 3, 231–259. ANSP 200486, 1, 210. *Sternarchella sima*: ANSP 192108, 2, 145–157. USNM 373114, 8, 2 CS, 136–158. *Sternarchogiton labiatus*: ANSP 200404, 2, 164–173. ANSP 200489, 1, 176. MUSM 59458, 12, 152–240. ANSP 198348, 2, 171–185. *Sternarchogiton nattereri*: ANSP 200393, 6, 89–200. ANSP 200447, 3, 161–204. MUSM 54644, 15, 40–210. *Sternarchogiton porcinum*: ANSP 200425, 3, 240–255. MUSM 54645, 10, 2 CS, 148–277. MUSM 54621, 2, 221–261. ANSP 198347, 19, 191–295. ANSP 185100, 49, 95–335. *Sternarchorhamphus muelleri*: MUSM 54642, 5, 244–362. *Sternarchorhynchus mormyrus*: MUSM 54650, 3, 2 CS, 205–258. ANSP 198402, 2, 246–300. *Tembeassu marauna*: MZUSP 48510, 1 HT, 194. MZUSP 23090, 2 PT, 188–196.

ACKNOWLEDGMENTS

We are grateful to J. Lundberg, C. Cox Fernandes (INPA), and all participants in the Calhamazon project for their collection efforts that laid the foundation for much of the present work on deep-channel fishes. Permits to export Peruvian specimens were provided by La Dirección Regional de Producción Loreto. Field work and specimen exports in Brazil were authorized via Expedição Científica-CNPq, the Instituto Brasileiro do Meio Ambiente e dos Recursos Naturais Renováveis, and a Material Transfer Agreement to C. Oliveira and the Instituto de Biociências de Universidade Estadual Paulista (UNESP). For assistance with cataloging museum specimens we thank M. Sabaj (ANSP) and H. Ortega (MUSM). We thank J. Craig, L. Kim, V. Tagliacollo, and P. Van der Sleen for assistance in field collections and B. Waltz for his helpful discussions of gymnotiform taxonomy and anatomy. We also thank Adam Summers for providing

access to a CT scanner at Friday Harbor Laboratories and Kazuyuki Muramatsu and Minoru Matsuzaka for providing photographs. This work was supported in part by United States National Science Foundation DEB 0614334, 0741450, and 1354511 to JSA.

REFERENCES

- **Albert JS.** Species diversity and phylogenetic systematics of American knifefishes (Gymnotiformes, Teleostei). Misc Publ Mus Zool Univ Mich. 2001; 190:1–127.
- **Albert JS, Campos-da-Paz R.** Phylogenetic systematics of Gymnotiformes with diagnoses of 58 clades: a review of available data. In: Malabarba L, Reis R, Vari R, Lucena Z, Lucena C, editors. Phylogeny and Classification of Neotropical Fishes. Porto Alegre: Edipucrs; 1998. p.419–46.
- **Albert JS, Cramton WGR.** A new species of electric knifefish, genus *Compsaraia* (Gymnotiformes: Apteronotidae) from the Amazon River, with extreme sexual dimorphism in snout and jaw length. Syst Biodivers. 2009; 7:81–92. https://doi.org/10.1017/S1477200008002934
- **Bernt MJ, Albert JS.** A new species of deep-channel electric knifefish *Compsaraia* (Apteronotidae, Gymnotiformes) from the Amazon River. Copeia. 2017; 105(2):211–19. https://doi.org/10.1643/CI-16-529
- **Bernt MJ, Crampton WGR, Orfinger AB, Albert JS.** *Melanosternarchus amaru*, a new genus and species of electric ghost knifefish (Gymnotiformes: Apteronotidae) from the Amazon Basin. Zootaxa. 2018; 4378(4):451–79. https://doi.org/10.11646/zootaxa.4378.4.1
- **Bernt MJ, Tagliacollo VA, Albert JS.** Molecular Phylogeny of the Ghost Knifefishes (Gymnotiformes: Apteronotidae). Mol Phylogenet Evol. 2019; 135:297–307. https://doi.org/10.1016/j.ympev.2019.02.019
- **Cox-Fernandes, C.** Diversity, distribution, and community structure of electric fishes (Gymnotiformes) in the channels of the Amazon River system, Brazil. [PhD Thesis]. Durham: Duke University; 1995.
- **Cox-Fernandes C, Lundberg JG, Riginos C.** Largest of all electric-fish snouts: hypermorphic facial growth in male *Apteronotus hasemani* and the identity of *Apteronotus anas* (Gymnotiformes: Apteronotidae). Copeia 2002; 2002(1):52–61. https://doi.org/10.1643/0045-8511(2002)002[0052:LOAEFS]2.0.CO;2
- **Cox-Fernandes C, Lundberg JG, Sullivan JP.** *Oedemognathus exodon* and *Sternarchogiton nattereri* (Apteronotidae, Gymnotiformes): the case for sexual dimorphism and conspecificity. Proc Acad Nat Sci Philadelphia. 2009; 158:193–207. https://doi.org/10.1635/053.158.0110
- **Crampton WGR.** The electric fish of the Upper Amazon: ecology and signal diversity. [PhD Thesis]. Oxford: University of Oxford; 1996.
- **Crampton WGR.** Effects of anoxia on the distribution, respiratory strategies and electric signal diversity of gymnotiform fishes. J Fish Biol. 1998a; 53(Supplement A):307–30. https://doi.org/10.1111/j.1095-8649.1998.tb01034.x
- **Crampton WGR.** Electric signal design and habitat preferences in a species rich assemblage of gymnotiform fishes from the Upper Amazon basin. An Acad Bras Cienc. 1998b; 70(4):805–47.
- **Crampton WGR.** Diversity and adaptation in deep channel Neotropical electric fishes. In: Sebert P, Onyango DW, Kapoor BG, editors. Fish Life in Special Environments. Enfield: Science Publishers Inc; 2007. p.283–39.
- **Crampton WGR.** An ecological perspective on diversity and distributions. In: Albert JS, Reis RE, editors. Historical biogeography of Neotropical freshwater fishes. Los Angeles: University of California Press; 2011. p.165–89.

- **Crampton WGR, Cella-Ribeiro A.** Apteronotidae. In: Queiroz L, Torrente-Vilara G, Ohara W, Pires T, Zuanon J, Doria C, editors. Peixes do rio Madeira. São Paulo: Dialeto Latin America Documentary; 2013. p.256–89.
- **Eigenmann CH, Allen WR.** Fishes of Western South America: 1. The Intercordilleran and Amazonian Lowlands of Peru. 2. The High Pampas of Peru, Bolivia and Northern Chile; With a Revision of the Peruvian Gymnotidae and of the Genus *Orestias*. Kentucky: University of Kentucky Press; 1942.
- **Eigenmann CH, Ward DP.** The Gymnotidae. Proc Wash Acad Sci. 1905; 7:157–85. Available from: https://www.jstor.org/stable/24525354
- **Evans KM, Waltz B, Tagliacollo VA, Chakrabarty P, Albert, JS.** Why the short face? Developmental disintegration of the neurocranium drives convergent evolution in Neotropical electric fishes. Ecol Evol. 2017; 7(6):1783–801. https://doi.org/10.1002/ece3.2704
- **Evans KM, Kim LY, Schubert BA, Albert JS.** Ecomorphology of Neotropical Electric Fishes: An Integrative Approach to Testing the Relationships between Form, Function, and Trophic Ecology. Integr Comp Biol. 2019; 1:1–16. https://doi.org/10.1093/iob/obz015
- **Ferraris CJ, Jr., Santana CD, Vari RP.** Checklist of Gymnotiformes (Osteichthyes: Ostariophysi) and catalogue of primary types. Neotrop Ichthyol. 2017; 15(1):e160067. https://doi.org/10.1590/1982-0224-20160067
- **Fink SV, Fink WL.** Interrelationships of the ostariophysan fishes (Teleostei). Zool J Linn Soc. 1981; 72(4):297–353. https://doi.org/10.1111/j.1096-3642.1981.tb01575.x
- **Hilton EJ, Cox-Fernandes C, Sullivan JP, Lundberg JG, Campos-da-Paz R.** Redescription of *Orthosternarchus tamandua* (Boulenger, 1898) (Gymnotiformes, Apteronotidae), with reviews of its ecology, electric organ discharges, external morphology, osteology, and phylogenetic affinities. Proc Acad Nat Sci Philadelphia. 2007; 156(1):1–25. https://doi.org/10.1635/0097-3157(2007)156[1:ROOTBG]2.0.CO;2
- **Hilton EJ, Cox-Fernandes C.** Identity of "*Apteronotus*" *bonapartii* (Castelnau, 1855), a sexually dimorphic South American knifefish from the Amazon, with notes on its cranial osteology and on the taxonomic status of "*Apteronotus*" *apurensis* Fernández-Yépez, 1968 (Gymnotiformes, Apteronotidae). Proc Acad Nat Sci Philadelphia. 2017; 165(1):91–103. https://doi.org/10.1635/053.165.0109
- **Janzen F.** Molecular Phylogeny of the Neotropical Knifefishes of the Order Gymnotiformes (Actinopterygii). [Master Dissertation]. Toronto: University of Toronto; 2016. Available from: http://hdl.handle.net/1807/80484
- **Lopez-Rojas H, Lundberg JG, Marsh E.** Design and operation of a small trawling apparatus for use with dugout canoes. N Am J Fish Manag. 1984; 4(3):331–34. https://doi.org/10.1577/1548-8659(1984)4%3C331:DAOOAS%3E2.0.CO;2
- **Mago-Leccia F.** Los Peces de la Familia Sternopygidae de Venezuela. Acta Cient Venez. 1978; 29(Supplement 1):1–89.
- **Mago-Leccia F.** Electric fishes of continental waters of America. Caracas: Biblioteca de la Academia de Ciencias Fisicas, Matematicas y Naturales; 1994.
- **Myers GS.** A new genus of gymnotid eels from the Peruvian Amazon. Proc Biol Soc Wash.1936; 49:115–16.
- Sabaj MH. Standard symbolic codes for institutional resource collections in herpetology and ichthyology: an Online Reference. Version 6.5 [Internet]. Washington; 2016. Available from: http://www.asih.org
- **Santana CD, Crampton WGR.** Revision of the deep-channel electric fish genus *Sternarchogiton* (Gymnotiformes: Apteronotidae). Copeia. 2007; 2007(2):387–402. https://doi.org/10.1643/0045-8511(2007)7[387:ROTDEF]2.0.CO;2
- **Silva FHR, Pieczarka JC, Cardoso AL, Silva PC, Oliveira JA, Nagamachi CY.** Chromosomal diversity in three species of electric fish (Apteronotidae, Gymnotiformes) from the Amazon Basin. Genet Mol Biol. 2014; 37(4):638–45. https://doi.org/10.1590/S1415-47572014005000018

- **Smith AR, Proffitt MR, Ho WW, Mullaney CB, Maldonado-Ocampo JA, Lovejoy NR, Alves-Gomes JA, Smith GT.** Evolution of electric communication signals in the South American ghost knifefishes (Gymnotiformes: Apteronotidae): A phylogenetic comparative study using a sequence-based phylogeny. J Physiol Paris. 2016; 110(3):302–13. https://doi.org/10.1016/j.jphysparis.2016.10.002
- **Tagliacollo VA, Bernt MJ, Craig JM, Oliveira C, Albert JS.** Model-based total evidence phylogeny of Neotropical electric knife fishes (Teleostei, Gymnotiformes). Mol Phylogenet Evol. 2016; 95:20–33. https://doi.org/10.1016/j.ympev.2015.11.007
- **Taylor WR, Van Dyke GC.** Revised procedures for staining and clearing small fishes and other vertebrates for bone and cartilage study. Cybium. 1985; 9(2):107–19.
- **Weitzman SH.** Osteology and evolutionary relationships of the Sternoptychidae, with a new classification of stomiatoid families. Bull Am Mus Nat Hist. 1974; 153(3):139–478. Available from: http://hdl.handle.net/2246/1139

AUTHOR CONTRIBUTIONS

Maxwell J. Bernt: Conceptualization, Data curation, Formal Analysis, Investigation, Methodology, Visualization, Writing (original draft) and Writing (review & editing).

Aaron H. Fronk: Conceptualization, Data curation, Formal Analysis, Investigation.

Kory M. Evans: Data curation, Methodology.

James S. Albert: Project administration, Supervision, Visualization and Writing (review & editing).

ETHICAL STATEMENTS

Written consent for all project activities was approved by the University of Louisiana at Lafayette Institutional Animal Care and Use Committee (IACUC) #2010-8717-064 for all activities related to this article.

COMPETING INTERESTS

Not applicable.

HOW TO CITE THIS ARTICLE

- **Bernt MJ, Fronk AH, Evans KM, Albert JA**. A redescription of deep-channel ghost knifefish, *Sternarchogiton preto* (Gymnotiformes: Apteronotidae), with assignment to a new genus. Neotrop Ichthyol. 2020; 18(1):e190126. https://doi.org/10.1590/1982-0224-2019-0126

Neotropical Ichthyology

OPEN ACCESS

This is an open access article under the terms of the Creative Commons Attribution License, which permits use, distribution and reproduction in any medium, provided the original work is properly cited.

Distributed under
Creative Commons CC-BY 4.0

© 2020 The Authors.
Diversity and Distributions Published by SBI

Official Journal of the
Sociedade Brasileira de Ictiologia
SBI